A STUDY ON NONLINEAR PHYSICAL PROBLEMS: NEW SOLUTIONS AND APPLICATIONS

A THESIS
SUBMITTED FOR THE DEGREE OF
DOCTOR OF PHILOSOPHY

By

Thokala Soloman Raju

SCHOOL OF PHYSICS
UNIVERSITY OF HYDERABAD
HYDERABAD 500 046, INDIA
SEPTEMBER 2003

CERTIFICATE

This is to certify that the work embodied in this thesis entitled "A STUDY ON NONLINEAR PHYSICAL PROBLEMS: NEW SOLUTIONS AND APPLICATIONS", has been carried out by Mr. T. Soloman Raju, under my supervision and the same has not been submitted in whole or part for a degree in any University.

Dr. PRASANTA K. PANIGRAHI

DEAN

SCHOOL OF PHYSICS

DEAN
School of Physics
University of Hyderabad
Hyderabad-500 046, INDIA

To

My Parents

Contents

Acknowledgements

It gives me an immense pleasure to express my deep sense of gratitude to my thesis supervisor, Dr. Prasanta K. Panigrahi for giving me an opportunity to work with him for my doctoral thesis. I profusely thank him for his excellent guidance, infinte patience, and encouragement throughout the pursuit of this work. My long association with him really propelled the real researcher in me to go ahead with the study of various nonlirieai' systems we have dealt with in this thesis. His killing instinct for cranking out the solutions for some of the toughest problems truly stirred me up to find some new solutions of various nonlinear equations. His interest in interdisciplinary subjects and ability to be successful astonishes me a lot. 1 also thank him for his wonderful teaching during my M.Phil., course work and subsequent years.

I am grateful to Prof. Chaturvedi, for being my In-charge supervisor and Prof. Srinivasan, for his kindness, during the time of submission of my thesis.

I owe an indebtedness to Prof. A. Khare, for many useful discussions and suggestions, during my visit to the Institute of Physics, Bhubaneswar.

1 am truly thankful to Dr. C. Nagaraja Kumar, who introduced me to this exciting field of "Solitons" in my first year of graduation. I have been greatly benifitted by his inspiring collaboration.

I am thankful to the former Deans of School of Physics; Profs. K.N. Shrivastava, S.N. Kaul, and the present Dean, Prof. V.S.S. Sastry, for providing the necessary facilities, to complete the thesis work.

wishes for this newly wed couple.

Last but not the least, I appreciate the fervent prayer support of my wife, Mrs. Swaroopa Rani, and my son, Jesse (Sharon Raju). At the time of finishing of the writing of this thesis, my daughter baby Nancy has been added into our family.

Above all, I extol the name of my Lord and Savior, Jesus Christ, for fulfilling His promise," ...he who began a good work in you will carry it on to completion until the day of Christ Jesus", (Phillippians 1:6).

Thokala Soloman Raju

Abstract

The common theme of this thesis is *nonlinearity*. Order parameters in models exhibiting phase transitions e.g., Bose-Einstein condensates, electric field in a nonlinear medium are some of the well-known examples of nonlinear systems in physics. These and other nonlinear dynamical systems, appearing in various physical problems, are the focus of our study here.

We start with the nonlinear Schrödinger equation (NLSE), with an external source. The externally driven NLSE has manifested in diverse areas of physics. For example, charge density waves, long Josephson junctions, plasma driven by rf fields, and optical twin-core fibers are governed by this nonlinear equation. We provide an exact mapping, through a *fractional transformation*, which connects the solutions of the NLSE, phase-locked with a source, to the elliptic functions satisfying $f'' \pm af \pm A f^3 - 0$. The solutions are *necessarily* of the rational type, containing both trigonometric and hyperbolic types, as special cases. Externally induced soliton trains, pulse and singular solutions are obtained. So far, no exact solutions have been found for this system; although a number of perturbation studies have been carried out around the familiar soliton solutions of the NLSE. We then numerically check the stability of some of these solutions through a powerful numerical technique, the semi-implicit Crank-Nicolson finite difference method. We have also analyzed the NLSE, with damping, in the presence of a space-time dependent source. The exact solutions may find applications in the recently developed method of dispersion management.

We then study solitary wave solutions, having strictly finite extent, the so called compact on solutions, in various integrable systems, possibly with modifications. With the help of the periodic solutions of modified Korteweg de-Vries (MKdV) and a host of other nonlinear equations, we point out that compacton type solutions can exist in these systems, provided appropriate sources are included.

The two-species Bose-Einstein condensates (TBEC), with the order parameter equations of the coupled NLSE type, are then analyzed for the presence of the solitary wave solutions. We study both the weakly and strongly coupled regimes, the latter being treated numerically. Solitary wave solutions of the TBEC, exhibiting a number of interesting properties, have been obtained.

The chiral order parameter having 0(4) symmetry, where the dynamical system is governed by a nonlinearity of the NLSE type, is then studied, keeping in mind the disoriented chiral condensate (DCC). These are space-time domains, where the order parameter can orient along a direction different from the low-energy vacuum direction. The possibility of DCC formation has aroused considerable interest in recent times. We find shape preserving solutions, describing DCC-type phenomena, in the quenching scenario. We then analyze the dynamics of the phase of the chiral order parameter, in the presence of the symmetry breaking term in the Hamiltonian, responsible for the pion masses. This was done in the regime, when the amplitude of the order parameter, takes a constant value. The relevant equation of motion in this case is the sine-Gordon equation. We find clusters of DCC, due to the nontrivial dynamics of the phase, under the condition of boost invariance. The behavior of the soliton solutions of the sine-Gordon equation, when allowed to expand into higher dimensions, is then studied. The physical picture being, the initial formation of these solitons in $(1+1)$-dimensions due to the pancake type geometry of the colliding heavy nuclei, subsequently expanding into the transverse dimensions. It

was numerically found that, the soliton solutions, which may be thought of as DCC-type domains, slowly destabilize in higher dimensions, leading to coherent particle production.

Chapter 1

Introduction

Nonlinear equations are ubiquitous in diverse branches of science. In physics, the well-known nonlinear Schrodinger equation (NLSE) [1] manifests in nonlinear fiber-optics [2, 3, 4] and with an appropriate potential as Gross-Pitaevskii (GP) equation in Bose-Einstein condensates [5]. The KdV, MKdV, and Boussinesq equations routinely appear in hydrodynamics and plasma physics [6]. The sine-Gordon equation and its variants manifest in Josephson junction arrays and charge density waves. By now, there are more than hundred nonlinear equations, for which solitary waves exist as solutions. A number of these equations are integrable in the Liouville sense; for these systems, an infinite number of conserved quantities exist, which are in involution. The integrability of these equations lead to extremely interesting properties for their solutions, the so called solitons. For example, the KdV solitons having higher amplitudes, move faster and overtake the solitons with lower amplitudes, and vice-versa for Boussinesq equation. However, in the process, the solitons remain unaffected.

Solitons can be localized or may appear as pulse trains; however, in both these cases, the nonlinearity and dispersion delicately balance each others' effect for these self-similar waves to exist. The subject of solitons in integrable models is well studied; the solitons have also been generated in controlled experiments [4, 7, 2]. Finding exact solutions, in particular,

traveling wave solutions of these nonlinear equations is an active research area. Many explicit methods have been introduced in the literature for the same purpose. Some of these methods are Backlund transformation, generalized Miura transformation, Darboux transformation, Cole-Hopf transformation, Lax pair approach, Painlevé analysis, Hirota-bilinear method, etc.

In a number of situations modifications of these integrable systems appear in physical problems, for which solitary wave solutions may exist. For example, externally driven NLSE has appeared in various physical problems. Although, perturbative treatment around the soli ton solution of NLSE has yielded a number of interesting insights, exact solutions of the complete equation will undoubtedly shed considerable light on the role of the source term. A significant portion of this thesis is devoted to the exact solutions of the same. We employ a fractional transformation to connect the elliptic functions to the solutions of the NLSE, phase locked with a source. Fractional linear transformations have been used extensively in case of linear differential equations. For example, the well-known Riemann equation and its solutions can be connected with the hypergeometric equation, through a bilinear transformation. It is interesting to find that a similar transformation can be profitably used to map the NLSE with a source to the equation with elliptic functions as solutions.

It is well-known in the soli ton literature, that a number of integrable equations can be transformed into the equation of the elliptic functions. The doubly periodic Jacobi elliptic functions, interpolate between trigonometric functions and the hyperbolic functions, through different values of the modulus parameter. The solutions of these nonlinear equations obtained in the form of elliptic functions yield, both localized soliton solutions, as well as the pulse train solutions possessing periodicity.

The obtained solutions of the NLSE with a source are necessarily of the rational form and have both trigonometric and hyperbolic pulse type

solutions. Some of them can also be singular. We have also successfully implemented a fractional transformation to find the solutions of the NLSE in an opaque medium, interacting with a space-time dependent source. In light of the tremendous interest in the dispersion managed solitons in optical fibers, the solitary wave solutions found in this case, mounted on a space-time dependent source, may find applications in soliton based communication systems [8]. We have also used this transformation to find rational solutions of the Boussinesq equation.

In recent times, a class of solutions of nonlinear equations called compactons, have attracted much attention. These are solitary wave solutions, having strictly finite extent. It will be worth-while to know, if modifications of some of these integrable equations may lead to compacton type solutions. We analyze MKdV and NLSE equations, and show that it is indeed possible to obtain compacton solutions, provided appropriate sources are included.

The physics of Bose-Einstein condensate and nonlinear optical systems share a number of similarities. The same NLSE, coupled with different types of potentials, can describe the dynamics of the Bose-Einstein condensates [5]. In light of the experimental observations of solitons and solitary waves in one component BEC, we carry out an extensive study of the TBEC for the existence of similar solutions. The TBEC reveal modulational instability and autocorrelation traces, akin to ones in laser systems [2].

Noticing that, the NLSE type nonlinearity appears in the description of the chiral order parameter, we then employ some of the above techniques for the description of DCC. As has been mentioned earlier DCC refers to domains in the chiral order parameter which are misaligned with respect to the vacuum direction.

In the following chapter, we map the solutions of the NLSE phase locked with a source to the elliptic functions satisfying; $f'' \pm af \pm A f^3 = 0$, through a *fractional transformation*. Here a, and A are real. We study a wide class

of traveling wave solutions, which are necessarily of rational form. It is worth emphasizing that the solutions are nonperturbative in nature. They include trigonometric and hyperbolic rational solutions, some of which may be singular. By using the semi-implicit Crank-Nicholson finite difference method, we have shown that the periodic solutions obtained in this procedure are stable. It should be noted that, the presence of a source term makes the numerical simulations quite nontrivial. The solutions are also studied in the presence of damping and time dependent coupling and dispersion.

In Chapter 3, we extend the use of the *fractional transformation,* that has been quite handy in finding the exact solutions of NLSE, phase-locked with a source, to other nonlinear equations. The goal is to look for the possibilty of solutions of strictly finite size, the so called compactons in these nonlinear systems. For that purpose, we first find exact traveling wave solutions in terms of Jacobi elliptic functions. The numerical simulations revealed that the rational, periodic solutions of MKdV, after some evolutions develop instability. We also found rational solutions of Boussinesq equation, using the *fractional transformation.* We then investigated the possibility of compactifying the periodic solutions of NLSE, MKdV, and higher order KdV-like equations. It was found that, in the case of MKdV, the periodic solution can be a compacton, only in the presence of a delta function-like source, the NLSE also needs to be appended with a suitable source, for a compacton type solution to exist.

In Chapter 4, we have explored the dynamics of two-species BEC by coupled NLSE, using the mean field approximation. In particular, the soliton and solitary wave solutions are studied in detail. It should be pointed out that solitons and soliton trains have been seen experimentally in single component BEC. In view of the experimental results reported for the two component BEC in ^{87}Rb, ^{41}K-^{87}Rb, and ^{7}Li-^{133}Cs, we hope that the exact solutions found in our work, may find applications. There are two regimes we

have considered for the coupling parameters. In the so called weak limit, we could find exact solutions of the two-coupled Gross-Pitaev ski equations, in terms of cnoidal functions. Bright, and dark solitons are found in this limit. Chirped pulses are obtained as exact solutions. We also carry out extensive numerical simulations, in this regime. In the strong coupling domain, we have numerically solved coupled GP equations; both for the attractive and repulsive cases. In the attractive case, chirping has been observed during numerical evolution, for appropriate values of the chemical potential. Interestingly, for one particular set of the parameter values, for one of the species, we observed traces of auto correlation, akin to a two laser system, due to modulational instability; the other one shows oscillatory behavior.

We have conducted analytical and numerical studies regarding the possibility of formation of disoriented chiral condensate (DCC) in the non-equilibrium picture, in Chapter 5. We start with the linear sigma model Lagrangian with an explicit symmetry breaking term, responsible for the pion mass and show that this can be reduced to the sine-Gordon (SG) equation under appropriate conditions. Both boost invariant and non-invariant solutions have been studied and their relevance for DCC pointed out. We present exact traveling wave solutions of the linear sigma model, these and the solitary wave solutions of the SG model can describe domains of DCC. We performed numerical simulations for both linear sigma model and the SG model in proper-time and pseudo-rapidity variables. Also, the space-time evolution of domains, under SG equation, is carried out using centered finite difference method.

References

[1] V.E. Zakharov and A.B. Shabat, Sov. Phys. JETP 34, 62-69 (1972).

[2] G.P. Agrawal, *Nonlinear Fiber optics* (Academic Press, Boston, 1989).

[3] A. Kumar, Phys. Rep. **187,** 63-108 (1990).

[4] A. Hasegawa, *Optical Solitons in Fibers* (Springer-Verlag, New York, 1990).

[5] C.J. Pethick and H. Smith, *Bose-Einstein Condensation in Dilute Gases* (Cambridge University Press, Cambridge, England, 2002) and references therein.

[6] A. Scott, *Nonlinear Science: emergence and dynamics of coherent structures* (Oxford University Press, Oxford, 1999).

[7] J.S. Russell, Br. Ass. Adv. Sci. Rep. 14, 311-392 (1844).

[8] A. Hasegawa and Y. Kodama, *Solitons in Optical Communications* (Oxford University Press, Oxford, 1995).

Chapter 2

The Nonlinear Schrodinger equation and sources

It has been well established that the nonlinear Schrodinger equation (NLSE) describes a wide class of physical phenomena e.g., modulational instability of water waves, propagation of heat pulses in anharmonic crystals, helical motion of a very thin vortex filament, nonlinear modulation of collision-less plasma waves, and self trapping of a light beam in a color dispersive system [1]. In optical fibers, the solitons of the NLSE provide a secure means to carry bits of information over many thousands of kilometers [2]. In many of these examples the equation appears as an asymptotic limit for a slowly varying dispersive wave envelope propagating through nonlinear medium. When termed as Gross-Pitaevskii equation; the NLSE with an appropriate potential can be utilized to describe the dynamics of the Bose-Einstein condensate, both with the attractive and repulsive nonlinearities. It is our objective in this chapter to present the solutions of the NLSE with an external source and a gain or lossy term, and study the numerical stability of some of the solutions. Like KdV equation, the NLSE is a generic wave equation, arising in the study of unidirectional propagation of wave packets in a dispersive, energy conserving medium at the lowest order of nonlinearity.

2.1   The nonlinear Schrodinger equation

In certain dielectric materials, the refractive index increases in proportion to the square of the electric field, this property is known as Kerr effect. Then the refractive index can be written as

$$n = n_s(\omega) + n_2|E|^2.$$

Consider an electromagnetic wave (in a scalar form) represented by the function:

$$\psi = a(z,t)e^{i(\omega_s t - k_s z)}, \tag{2.1}$$

where $a(z, t)$ is a dimensionless complex amplitude representing the slowly varying envelope of the wave and ω_s is the wave central frequency ($k_s = n\omega_s/c$). The wave intensity is given by $I = I_c \setminus \psi(z,t) \mid^2$, where I_c is a constant. The optical Kerr effect increases the refractive index by the quantity $\delta n = n_2 I$, where n_2 is the nonlinear refractive index coefficient. We assume that near the central frequency of the wave, the following dispersion relation holds:

$$k(\omega) = k_s + (\omega - \omega_s)(\frac{\partial k}{\partial \omega})_{\omega_s} + \frac{(\omega - \omega_s)^2}{2}(\frac{\partial^2 k}{\partial \omega^2})_{\omega_s} +$$
$$+ \frac{(\omega - \omega_s)^3}{3!}(\frac{\partial^3 k}{\partial \omega^3})_{\omega_s} + \cdots + k_2 I + I(\omega - \omega_s)(\frac{\partial k_2}{\partial \omega})_{\omega_s} + \cdots \tag{2.2}$$

Equation (2.2) is a Taylor development of the wave vector near ω_s, with the addition of the effect of nonlinearity $\delta k = k_2 I$ with $k_2 = n_2\omega_s/c$. In this equation, if we replace the derivatives k', k'' etc. through their relationship to the group velocity, $v_g = \frac{\partial \omega}{\partial k}$, then we arrive at:

$$\frac{1}{v_g} = \frac{\partial k}{\partial \omega} = (\frac{\partial k}{\partial \omega})_{\omega_s} + (\omega - \omega_s)(\frac{\partial^2 k}{\partial \omega^2})_{\omega_s} +$$
$$+ \frac{(\omega - \omega_s)^2}{2}(\frac{\partial^3 k}{\partial \omega^3})_{\omega_s} + \cdots + I(\frac{\partial k_2}{\partial \omega})_{\omega_s} + \cdots$$
$$\equiv k' + \frac{(\omega - \omega_s)}{\cdots} \cdot k'' + \frac{(\omega - \omega_s)^2}{2}k''' + \cdots$$
$$+ Ik_2' + \cdots \tag{2.3}$$

At the frequencies of interest for solitons in single-mode fibers, the terms in k'' and $k_2 I$ in Eq. (2.2) have comparable magnitudes, while the higher order terms in k''' and Ik'_2 are like small perturbations. Thus Eq. (2.2) can be approximated by:

$$\triangle k \approx \triangle\omega k' + \frac{\triangle\omega^2}{2}k'' + k_2 I,$$ **(2.4)**

with $\triangle k = k - k_s$, and $\triangle\omega = \omega - \omega_s$. From Eq. (2.3), we find that,

$$k'' \approx \frac{\partial}{\partial\omega}\left(\frac{1}{v_g}\right) = -\frac{1}{v_g^2}\frac{\partial v_g}{\partial\omega}$$ (2.5)

which shows that k'' is the dispersion of the wave's group velocity.

We now consider the Fourier transform of the envelope function:

$$\tilde{\psi}(\triangle k, \triangle\omega) = \int \psi(z,t)e^{i(\triangle\omega t - \triangle kz)}dt dz,$$ **(2.6)**

$$\psi(z,t) = \frac{1}{(2\pi)^2}\int \tilde{\psi}(\triangle k, \triangle\omega)e^{-i(\triangle\omega t - \triangle kz)}d(\triangle\omega)d(\triangle k).$$ **(2.7)**

From Eqs. (2.6) and (2.7) we can show that the quantities $\partial\psi/\partial z = i\triangle k\psi$ and $\partial\psi/\partial t = -i\triangle\omega\psi$ are the Fourier transforms of $i\triangle k\tilde{\psi}$ and $-i\triangle\omega\tilde{\psi}$, respectively. Thus $\triangle k$, $\triangle\omega$ can be put into the form of operators $-i\partial/\partial z$, $i\partial/\partial t$. By substituting these operator forms into Eq. (2.4), we get:

$$-i\frac{\partial}{\partial z} \approx ik'\frac{\partial}{\partial t} - \frac{1}{2}k''\frac{\partial^2}{\partial z^2} + k_2 I.$$ (2.8)

Applying Eq. (2.8) to the wave envelope $\psi(z,t)$ and using $I = I_c \mid \psi(z,t) \mid^2$, we obtain:

$$i\frac{\partial\psi}{\partial z} + ik'\frac{\partial\psi}{\partial t} - \frac{k''}{2}\frac{\partial^2\psi}{\partial t^2} + k_2 I_c \mid \psi(z,t)\mid^2 \psi \approx 0$$ (2.9)

Equation (2.9) can be transformed to correspond to a retarded time frame and be made dimensionless through the following substitutions: $\tau = (t - k'z)/t_c$, $\chi = z/z_c$, where t_c, z_c are constants with dimensions of time and space, respectively. Hence, from Eq. (2.9), we get

$$-i\frac{t_c^2}{k'' z_c}\frac{\partial\psi}{\partial\chi} + \frac{1}{2}\frac{\partial^2\psi}{\partial\tau^2} - \frac{t_c^2}{k''}k_2 I_c \mid \psi \mid^2 \psi = 0.$$ (2.10)

If the constants are defined as below, $\frac{t_c^2}{z_c} = -k''$ and $z_c = \frac{1}{k_2 I_c}$, then the above equation can be cast into the canonical form:

$$i\frac{\partial \psi}{\partial \chi} + \frac{1}{2}\frac{\partial^2 \psi}{\partial \tau^2} + \mid \psi \mid^2 \psi = 0. \tag{2.11}$$

This is the celebrated *nonlinear Schrodinger equation*. It is so called, because of its similarity in appearance with the Schrodinger equation in quantum theory. In the case where the medium has gain or loss, a term $-i\Gamma\psi$ with $\Gamma = z_c g/2$ must be added to the left-hand side of Eq. (2.11), where g is the net power gain coefficient:

$$i\frac{\partial \psi}{\partial \chi} + \frac{1}{2}\frac{\partial^2 \psi}{\partial \tau^2} + \mid \psi \mid^2 \psi - i\Gamma\psi = 0. \tag{2.12}$$

It is our goal in this thesis, to present the solitary wave solutions of the NLSE in the presence of a source, and also with dispersion managed lossy and gain parameters. Before going into the details of NLSE interacting with external sources, we concentrate on free NLSE.

The NLSE is a second order nonlinear partial differential equation, which can contain localized solitons as solutions. Zakharov and Shabat solved the NLSE by the aid of inverse scattering method [3]. It is interesting to notice that, the solitons emerge, when the nonlinearity balances the dispersion. Solitons are stable, localized waves that propagate in a nonlinear medium without spreading. Solitons may be either bright or dark, depending on the details of the governing equation. A bright soliton is a peak in the amplitude; a dark soliton is a notch with a characteristic phase step across it. In addition to its solitons, NLSE supports periodic waves and exact N-soliton solutions [4].

2.2 The solutions of NLSE in terms of Jacobi elliptic functions

For the purpose of illustration we solve below, the NLSE in terms of the elliptic functions. The intended solutions are the traveling wave solutions, which can exhibit chirping. The NLSE is given by

$$i\hbar\partial_t\psi + \frac{\hbar^2}{2m}\partial_x^2\psi + g\mid\psi\mid^2\psi = 0 \quad , \tag{2.13}$$

where g is real. In the scaled variables $y = \sqrt{\frac{2m}{\hbar^2}}x$, and $t = \frac{t'}{\hbar}$, Eq. (2.13) takes the form:

$$i\partial_t\psi + \partial_y^2\psi + g\mid\psi\mid^2\psi = 0 \quad . \tag{2.14}$$

Using the following ansatz,

$$\psi(y,t) = e^{i[\phi(\xi)-\omega t]}a(\xi) \quad , \tag{2.15}$$

where $\xi = \alpha(y - vt)$, we can separate the real and the imaginary parts of the equation. The imaginary part

$$-u\alpha a' + \alpha^2\psi''a + 2\alpha^2\psi'a' = 0 \quad , \tag{2.16}$$

can be straightforwardly solved to give

$$\psi' = \frac{u}{2\alpha} + \frac{P}{\alpha a^2} \quad , \tag{2.17}$$

where, P is the integration constant. For $P \neq 0$, the solutions exhibit chirping. For simplicity, we consider $P = 0$ in which case the real part is given by

$$\epsilon a + \alpha^2 a'' + ga^3 = 0 \ , \tag{2.18}$$

where $\epsilon = \frac{v^2}{4} - \omega$. The solutions of the above equation are the well-known elliptic functions. Below we tabulate a few cnoidal solutions of the above equation.

Table I. Various limits for the exact solutions of NLSE

Cnoidal function	Modulus parameter (m)	$a(\xi)$
$A\mathrm{cn}(\xi, m)$	1	$\sqrt{\frac{-2\epsilon}{g}}\,\mathrm{sech}(\xi)$
$A\mathrm{cn}(\xi, m)$	5/8	$\sqrt{\frac{-5\epsilon}{g}}\,\mathrm{cn}(\xi, m)$
$B\mathrm{sn}(\xi, m)$	1	$\sqrt{\frac{-\epsilon}{g}}\,\tanh(\xi)$
$B\mathrm{sn}(\xi, m)$	1/2	$\sqrt{\frac{-2\epsilon}{3g}}\,\mathrm{sn}(\xi, m)$
$C\mathrm{dn}(\xi, m)$	1/2	$\sqrt{\frac{-4\epsilon}{3g}}\,\mathrm{dn}(\xi, m)$

As is clear from the above solutions the signs of y (attractive and repulsive) and ϵ play crucial roles in finding the solutions. This fact will become more explicit as we will use the solutions of the above equation repeatedly in our derivations.

2.3 The NLSE equation with a source

In this section, we present a wide class of rational solutions of the NLSE with a source, using a fractional transformation (FT). The solutions of NLSE, phase locked with a source, are exactly connected to the elliptic functions. These are necessarily of the rational type and are nonperturbative in nature. The numerical simulations revealed that some of these solitary waves are stable. We also present an elegant numerical technique to test the numerical stability of these exact solutions.

Much attention has been paid to the study of the externally driven NLSE after the seminal work of Kaup and Newell [5]. This equation features

prominently in the problem of optical pulse propagation in asymmetric, twin-core optical fibers [6, 7, 8]; currently an area of active research. Of the several applications of an externally driven NLSE, perhaps the most important ones are to long Josephson junctions [9], charge density waves [10], and plasmas driven by rf fields [11]. The phenomenon of autoresonance [12], indicating a continuous phase locking between the solutions of NLSE and the driving field, has been found to be a key characteristic of this system. in the presence of damping, this dynamical system exhibits rich structure including bifurcation. This is evident from analyses around a constant background as well as numerical investigations [13, 14, 15]. Although NLSE is a well-studied integrable system [16], no exact solutions have so far been found for the NLSE with a source, to the best of the authors' knowledge. All the above inferences have been drawn through perturbations around solitons and numerical techniques.

In this chapter, we map *exactly,* the traveling wave solutions of the NLSE phase-locked with a source, to the elliptic functions, through the FT. It was found that the solutions are *necessarily* of the rational type, with both the numerator and denominator containing terms quadratic in elliptic functions, in addition to having constant terms. It is well-known that the solitary wave solutions of the NLSE [17, 8] are cnoidal waves, which contain the localized soliton solutions in the limit, when the modulus parameter equals one [19]. Hence, the solutions found here, for the NLSE with a source, are nonperturbative in nature. We find both bright and dark solitons as also singular ones. Solitons and solitary pulses show distinct behavior. In the case, when the source and the solutions are not phase matched, perturbation around these solutions may provide a better starting point.

For nonlinear equations, a number of transformations are well-known in the literature, which map the solutions of a given equation to the other [20, 21]. The familiar example being the Miura transformation [22], which

maps the solutions of the modified KdV to those of the KdV equation. To find static and propagating solutions, appropriate transformations have also been cleverly employed, to connect the nonlinear equations to the ones satisfied by the elliptic functions: $f'' \pm a/ \pm A^{\beta} = 0$. Here and henceforth, prime denotes derivative with respect to the argument of the function. Solitons and solitary wave solutions of KdV, NLSE, and sine-Gordon etc., can be easily obtained in terms of the elliptic functions in this manner.

Below, we consider the NLSE coupled to an external traveling wave field η:

$$i\hbar \partial_t q + \frac{\hbar^2}{2m}\partial_x^2 q + g\mid q\mid^2 q + \mu q - \eta = 0 \quad .$$

where g and μ are real. In the scaled variable; $y = \sqrt{\frac{2m}{\hbar^2}}x$, and $t = \frac{t'}{\hbar}$, the above equation takes the dimensionless form:

$$i\partial_t q + \partial_y^2 q + g\mid q\mid^2 q + \mu q - \eta = 0 \quad .$$

Using the following ansatz,

$$q(y,t) = e^{i[\psi(\xi)-\omega t]}a(\xi);$$

we derive the moving solutions of Eq. (2.19). Here $\xi = \alpha(y - vt)$, and choosing the source term as $\eta(\xi) = ke^{i[\psi(\xi)-\omega t]}$, we can separate the real and the imaginary parts of the equation as:

$$v\alpha a\psi' + (\mu - \omega)a - \alpha^2\psi'^2 a + \alpha^2 a'' + ga^3 - k = 0, \tag{2.20}$$

and

$$-v\alpha a' + \alpha^2\psi'' a + \alpha^2\psi' a' = 0 \quad , \tag{2.21}$$

where the primes denote the derivatives with respect to ξ variable. Equation (2.21) can be straightforwardly solved to give

$$\psi' = \frac{v}{2\alpha} + \frac{P}{\alpha a^2} \quad , \tag{2.22}$$

where P is the integration constant, which has been set to zero in the following. Thus the single nonlinear ordinary differential equation we have to solve is

$$\epsilon a + \alpha^2 a'' + g a^3 - k = 0 \quad , \tag{2.23}$$

with $\epsilon = \frac{v^2}{4} + \mu - \omega$.

2.4 Solitary wave solutions of the NLSE with a source

2.4.1 General solutions

We start with an ansatz solution of equation (2.23) of the form,

$$a(\xi) = \frac{A + B f^\delta(\xi, m)}{1 + D f^\delta(\xi, m)},$$

with δ taking integer values. After substitution, the coefficients of $f^n(\xi, m)$, for $n = 0,2,4,6$ etc., can be set to zero, to reduce the problem to a set of algebraic equations. Since the goal is to map the solutions of Eq. (2.23) to elliptic functions, use was made of the following relations for various derivatives of f; $f'' = f - f^3$, and $f'^2 = f^2 - \frac{1}{2}f^4 + 2E_0$, where E_0 is the integration constant. It was found that δ takes the unique value 2 for consistency. The consistency conditions will be solved below for specific choices of f. However, it is worth noticing that several interesting special cases already emerge from preliminary analysis.

Case(i):

For $A = 0$ and $B \neq 0$, we find that the solution is given by

$$a(\xi) = \frac{k/4E_0 f^2}{1 + (1/8E_0)f^2}.$$

Case(ii):

In another scenario, $B = 0$ and $A \neq 0$; the solution is

$$a(\xi) = \frac{2k}{1 - f^2},$$

which can be potentially singular. Although /, in principle, can be any of the twelve Jacobi elliptic functions, we concentrate primarily on: $cn(\xi, m)$, $dn(\xi, m)$, and $sn(\xi, m)$. The identities ($cn^2 = 1 - sn^2$, $dn^2 = 1 - rasn^2$) satisfied by these cnoidal functions come handy in the algebraic analysis. For definiteness, we start with $f = cn(\xi, m)$; then the coefficients of $cn^n(\xi, m)$, for $n = 0,2,4,6$ can be set to zero reducing the problem to a set of four algebraic equations as given below:

$$A\epsilon - 2\alpha^2(AD - B)(l - m) + gA^3 - k = 0, \tag{2.24}$$

$$2\epsilon AD + \epsilon B + 6\alpha^2(AD - B)D(l - m) -$$
$$4\alpha^2(AD - B)(2rn - 1) + 3gA^2B - 3kD = 0, \tag{2.25}$$

$$AeD^2 + 2\epsilon BD + 4\alpha^2(AD - B)D(2m......1) +$$
$$6\alpha^2(AD - B)m + 3gAB^2 - 3kD^2 = 0, \tag{2.26}$$

$$\epsilon BD^2 - 2\alpha^2(AD - B)Dm + gB^3 - kD^3 = 0. \tag{2.27}$$

We notice that in Eqs. (2.24)-(2.27), the free parameters are A, B, D, α, and the modulus parameter m. In what follows, we demonstrate, under various limits, how the imbalance between the group velocity dispersion of the slowly varying envelope mounted on a weakly varying carrier wave with the cubic nonlinearity can lead to solitary wave solutions in the presence of an appropriate source. These solutions may find applications in long distance optical communications [16]. First we analyze the general cases and then move on to the special ones.

From the consistency conditions, it is clear that when the source is switched off, the solitary wave envelope is not of a rational type. This is because, for $D - 0$, Eq. (2.27) yields $B = 0$. This indicates that, excluding a constant solution, there exists no other solution for Eq. (2.23). For

$AD = B$, it is observed that all the four equations are identical, a flat background solution is obtained. This shows that, $a(\xi) = A + B\mathrm{cn}^2(\xi, m)$, type of solutions do not exist for Eq. (2.23). Insead of cn, if one chooses *dn* or *sn* for f, the same scenario emerges. Hence, $a(\xi)$ is necessarily of the *rational* type. It should be noted that these are nonperturbative solutions, which can not be obtained from the elliptic function solutions of the NLSE given earlier, through perturbative means.

As mentioned earlier, the special cases lead to a number of interesting solutions. These contain both periodic and hyperbolic type solutions, some of which may be singular. We present them below, with the specifications for the regimes in which they exist.

2.4.2   Special solutions

Case(I): Trigonometric solution

For $A = 0$ and $m = 0$; we found that $\alpha^2 = -\epsilon/4$; hence, ϵ has to be negative, which puts restriction on v, μ, and ω. The parameters are also constrained as $\epsilon = (-\frac{27}{2} gk^2)^{\frac{1}{3}}$. Then we arrive at the periodic solution, for the attractive regime $[g > 0)$:

$$a(\xi) = (-\frac{2k}{\epsilon}) \frac{\cos^2(\xi)}{1 - \frac{2}{3}\cos^2(\xi)}. \tag{2.28}$$

This periodic solution is found to be stable, as evidenced from the numerical simulations to be given later in the text. It should be noted that for $B = 0$, no rational periodic solutions are possible.

Case(II): Hyperbolic solution

In this case, we find that for $A = 0$, no rational solutions exist. For $B = 0$, and $m = 1$; we found that $a^2 = \epsilon/4$. The parameters v, μ, and ω are related to the coupling strength as $\epsilon = (-\frac{27}{2} gk^2)^{\frac{1}{3}}$. This yields, the hyperbolic solution, for the repulsive scenario:

$$a(\xi) = (\frac{3k}{\epsilon}) \frac{1}{1 - \frac{3}{2}\mathrm{sech}^2(\xi)}, \tag{2.29}$$
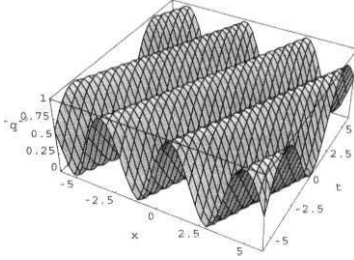
Figure 2.1: Plot depicting a periodic solution given in Eq. (2.33).

which is a singular one. The singularity here may correspond to extreme increase of the field amplitude due to self-focussing. We give below an example of a nonsingular solution. We take $m = 1$ and $AD - B = 1$ for simplicity. From Eq. (2.27), we determine the value of α^2 as

$$\alpha^2 = \frac{1}{2D}[\epsilon BD^2 + gB^3 - kD^3].$$ (2.30)

For $B - 0$, we immediately arrive at a nonsingular solution

$$a(\xi) = (\frac{3k}{\epsilon})\frac{1}{1 + (\frac{\epsilon}{3k})\text{sech}^2(\xi)},$$ (2.31)

subject to the following constraints: (i) for k positive, $\epsilon > 0$, hence $\omega < \frac{}{4} + \mu$, and (ii) for k negative, $\epsilon < 0$, hence $\omega > \frac{v^2}{4}4\,\mu$.

Case(III): Pure cnoidal solutions

Below we give another periodic solution, where the modulus parameter takes a specific value. In this case, $A = 0$, $D = 1$, and $m = 5/8$; here $\alpha^2 = \epsilon/2(3 - 2m)$. The parameters v,μ, and UJ are related to the coupling strength as $\epsilon = 7(-\frac{gk^2}{18})^{\frac{1}{3}}$. This solution corresponds to the repulsive regime. It should be pointed out that in this case the solution is unique, as noticed

above, various parameters are also related in this case. This gives rise to the cnoidal solution,

$$a(\xi) = (\frac{k}{\epsilon})(\frac{3-2m}{1-m})\frac{\text{cn}^2(\xi,m)}{1+\text{cn}^2(\xi,m)}. \tag{2.32}$$

For $A = 0$ and $m = 1/2$; it is found that $\alpha^2 = \epsilon/2\sqrt{3}$ and $\epsilon = (-27gk^2)^{\frac{1}{3}}$. This results in another cnoidal solution:

$$a(\xi) = (\frac{2\sqrt{3}k}{\epsilon})\frac{\text{cn}^2(\xi,m)}{1+\frac{1}{\sqrt{3}}\text{cn}^2(\xi,m)}. \tag{2.33}$$

For the sake of clarity, the above obtained solutions are tabulated below.

Table I. Various limits for the exact solutions of NLSE with a source

Modulus parameter (m)	A	B	D	$a(\xi)$
0	0	$-2k/\epsilon$	$-2/3$	$(-\frac{2k}{\epsilon})\frac{\cos^2(\xi)}{1-\frac{2}{3}\cos^2(\xi)}$
1	$3k/\epsilon$	0	$-3/2$	$(\frac{3k}{\epsilon})\frac{1}{1-\frac{3}{2}\text{sech}^2(\xi)}$
5/8	0	$14k/3\epsilon$	1	$(\frac{k}{\epsilon})(\frac{3-2m}{1-m})\frac{\text{cn}^2(\xi,m)}{1+\text{cn}^2(\xi,m)}$
1/2	0	$2\sqrt{3}k/\epsilon$	$1/\sqrt{3}$	$(\frac{2\sqrt{3}k}{\epsilon})\frac{\text{cn}^2(\xi,m)}{1+\frac{1}{\sqrt{3}}\text{cn}^2(\xi,m)}$

We now give some general localized solutions. Taking $m = 1$ ($\text{cn}(\xi,1) = \text{sech}(\xi)$), with the parameter values $A = 1$, $B - S$, and $D = 1$ S we obtain

$$\rho(\xi) = \frac{1+\delta\text{sech}^2(\xi)}{1+\Gamma\text{sech}^2(\xi)}; \tag{2.34}$$

here the amplitude, width, and velocity are related as,

$$\delta = -(Q + \sqrt{Q^2 - 4PR})/2Q,$$

with $Q = \epsilon - 2\alpha^2 - 3k$, $P = 2\epsilon - 3k$, $R = -k - 2\alpha^2$ and $\Gamma = \backslash + 8$. Hence, the width rv is the only independent parameter. As the above form of the solution indicates, both nonsingular and singular solitons are possible solutions depending on the values of ϵ, and the source strength k.

2.5   Numerical results

Since the localized solitons are usually robust, we have performed numerical simulations to check the stability of the solutions pertaining to Case(I), i.e., the trigonometric solution. It is worth pointing out that the numerical techniques based on the fast Fourier transform (FFT) are expensive as they require the FFT of the external source. Hence, we have used the **Crank-Nicolson** finite difference method to solve the NLSE with a source, which is quite handy, and unconditionally stable. Below a detailed description of the algorithm is given. We write $q — R + iI$, where R and $/$ are real-valued functions. Then the NLSE with a source is equivalent to the following coupled system of equations:

$$\partial_t R = -\frac{1}{2}\partial_x^2 I - g(R^2 + I^2)I + k\sin(kx - \omega t),$$

(2.35)

and

$$\partial_t I = \frac{1}{2}\partial_x^2 R + g(R^2 + I^2)R - k\cos(kx - \omega t).$$

(2.36)

Euler algorithm:

The finite-difference scheme for the Eqs. (2.35) and (2.36) can be written as follows:

$$R_i^{n+1} = R_i^n - \frac{\Delta t}{2(\Delta x)^2}[I_{i+1}^n - 2I_i^n + I_{i-1}^n]-$$
$$g\Delta t[(R_i^n)^2 + (I_i^n)^2]I_i^n + k\Delta t\sin(kx - \omega t),$$

(2.37)

and
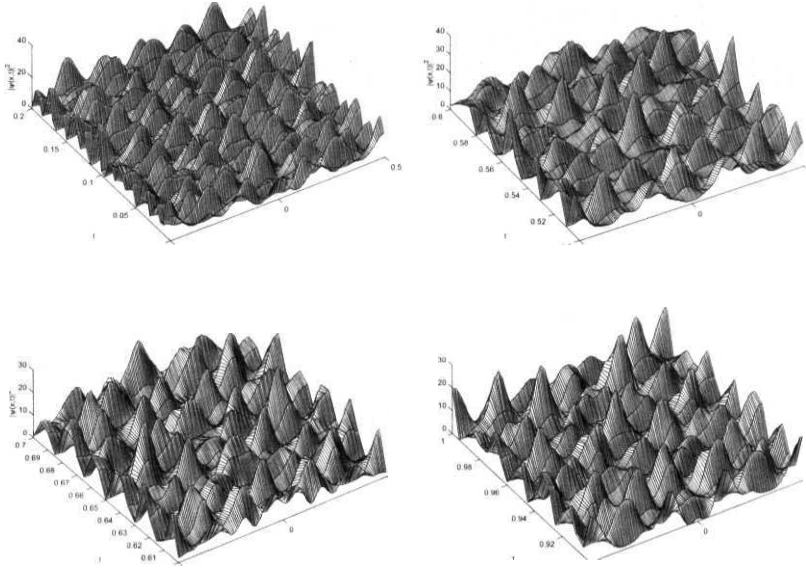
Figure 2.2: Plot depicting the evolution of the trigonometric solution, for various times.

$$I_i^{n+1} = I_i^n + \frac{\Delta t}{2(\Delta x)^2}[R_{i+1}^n - 2R_i^n + R_{i-1}^n] +$$
$$g\Delta t[(R_i^n)^2 + (I_i^n)^2]R_i^n - k\Delta t\cos(kx - \omega t). \qquad (2.38)$$

Second-order algorithm:

We present here, the semi-implicit CNFD for the NLSE in the presence of an external source. The recurrence relations for the Eqs. (2.35) and (2.36)

are written as:

$$R_i^{n+1} = R_i^n - \frac{\Delta t}{4(\Delta x)^2}[I_{i+1}^{n+1} - 2I_i^{n+1} + I_{i-1}^{n+1}] -$$
$$\frac{\Delta t}{4(\Delta x)^2}[I_{i+1}^n - 2I_i^n + I_{i-1}^n] - (g/2)\Delta t[(R_i^n)^2 +$$
$$(I_i^n)^2]I_i^n - (g/2)\Delta t[(R_i^n)(R_i^{n+1}) +$$
$$(I_i^{n+1})^2]I_i^{n+1} + k\Delta t\sin(kx - \omega t), \tag{2.39}$$

and

$$I_i^{n+1} = I_i^n + \frac{\Delta t}{4(\Delta x)^2}[R_{i+1}^{n+1} - 2R_i^{n+1} + R_{i-1}^{n+1}] +$$
$$\frac{\Delta t}{4(\Delta x)^2}[R_{i+1}^n - 2R_i^n + R_{i-1}^n] + (g/2)\Delta t[(R_i^n)^2 +$$
$$(I_i^n)^2]R_i^n + (g/2)\Delta t[(I_i^n)(I_i^{n+1}) +$$
$$(R_i^{n+1})^2]R_i^{n+1} - k\Delta t\cos(kx - \omega t). \tag{2.40}$$

Furthermore, R_i^n and I_i^n denote the approximation of the solution at $t = n\Delta t$, and $x_{final} = x_{initial} + ih$ with $h = \frac{x_{final} - x_{initial}}{N}$, where N is the total number of grid points. The initial conditions chosen from the exact solution are knitted on a lattice with a grid size $dx = 0.005$, and $dt = 5.0 \times 10^{-6}$. The simulations carried out indicate clearly that the above-mentioned solution is stable (Fig. 2.2). The initial and the boundary conditions are:

$$R_0^{n+1} = R_M^{n+1},$$

and

$$I_0^{n+1} = I_M^{n+1}.$$

If $i = N$, then

$$R_{N+1}^{n+1} = R_2^{n+1},$$

and for $i = 1$

$$R_{i-1}^{n+1} = R_{N-1}^{n+1}.$$

To summarize, we have used a fractional transformation to connect the solutions of the phase-locked NLSE with the elliptic functions, in an exact

manner. The solutions are necessarily of the rational type that contain solitons, solitary waves, as also singular ones. Our procedure is applicable, both for the attractive and repulsive cases. Because of their exact nature, these will provide a better starting point for the treatment of general externally driven NLSE. Considering the utility of this equation in fiber optics and other branches of physics, these solutions may find practical applications.

2.6 NLSE in opaque medium with distributed coefficients and an external source

In this section we present a wide class of rational and periodic solutions of the nonlinear Schrodinger equation with a source, in an opaque medium with distributed coefficients. As we will see below certain relationships between the coefficients and a particular type of source will lead to exact solutions. It should be noted that space and time are interchanged in the following equation as compared to the previous section, as is appropriate for an optical fiber.

The damped nonlinear Schrodinger equation, coupled to an external space-time dependent source with distributed coefficients can be written **as,**

$$i\Psi_z - \frac{\beta(z)}{2}\Psi_{\tau\tau} + \gamma(z) \mid \Psi \mid^2 \Psi = i\frac{g(z)}{2}\Psi + \eta e^{i\Phi(\tau,z)}. \tag{2.41}$$

It is assumed that the parameters β, γ, η, and g are all functions of the propagation distance z. The explicit relationships between them will be given below.

The damped NLSE, for which the distributed terms are independent of the propagation distance appeared in a variety of contexts: breathers in charge-density-wave materials in the presence of an applied ac field [5], breathers in long Josephson junctions [24], in easy-axis ferromagnets in

a rotating magnetic field [25, 26], and as solitons in the plasmas driven by rf fields [11, 27]. However, in recent years an important technology referred to as dispersion management (DM) has been developed by the researchers [28, 29]. DM means that optical fibers with sharply different dispersion characteristics, anomalous and normal, are combined together in subsections of the fiber and then this substructure is periodically repeated to cover the entire fiber length. DM tecnique is exploited profitably to enhance the power of the optical solitons, and reduce the effects of Gordon-Haus timing jitter [30]. Equation (2.41) describes the amplification or attenuation [for $g(z)$ is negative] of pulses propagating nonlinearly in a single mode fiber, where $\Psi(\tau, Z)$ is the complex envelope of the electric field in a comoving frame, r is the retarded time, $\beta(z)$ is the group velocity dispersion (GVD) parameter, $\gamma(z)$ is the nonlinearity parameter, and $g(z)$ is the distributed gain function. In the absence of a source, numerically it was shown that, in the case where the gain due to the nonlinearity and the linear dispersion balance with each other; equilibrium solitons will be formed[31]. Recently, V. I. Kruglov *et al* have reported exact self-similar solutions characterized by a linear chirp [32, 33]. Solitary wave solutions of this type of NLSE helps in analyzing the compression problem of the laser pulse in a dispersion decreasing optical fiber. Motivated by this work and our results on solutions of NLSE with a source, we analyze below the effects of the distributed coefficients and damping on the exact rational solutions of Eq. (2.41). It is hoped that, these solutions may find experimental realization, particularly in the solitary wave based communication links [8, 28].

By writing the complex function $\Psi(z, \tau)$ as

$$\Psi(z, \tau) = P(z, \tau)\exp[i\Phi(z, \tau)], \qquad (2.42)$$

where P and Φ are real functions of z and T; we look for the rational solutions of the NLSE assuming that the phase has the following quadratic

form:

$$(2.43)$$

Note that these solutions have a linear chirping. Now, Eqs. (2,42), (2.43) yield a self similar form of the amplitude:

$$P(z,\tau) = \frac{1}{\sqrt{1 - c_0 R(z)}} Q(\frac{\tau - \tau_c}{1 - c_0 R(z)}) \exp(\frac{1}{2} S(z)), \qquad (2.44)$$

where τ_c is the center of the pulse, and the functions $a(z)$, $c(z)$, $R(z)$ and $S(z)$ are given by

$$a(z) = a_0 - \frac{\lambda}{2} \int_0^z \frac{\beta(z')dz'}{(1 - c_0 R(z'))^2}, \qquad (2.45)$$

$$c(z) = \frac{c_0}{1 - c_0 R(z)}, \qquad (2.46)$$

$$R(z) = 2 \int_0^z \beta(z')dz', \qquad S(z) = \int_0^z g(z')dz', \qquad (2.47)$$

where a_0, A, and c_0 are the integration constants. Here, $\eta = \frac{\beta(z)}{2(1 - c_0 D(z))^{3/2}} \varepsilon$, and ε is the strength of the source. Furthermore, the function $Q(T)$ which determines the amplitude $P(z,\tau)$ in Eq. (2.44) can be found by solving the following nonlinear ODE

$$Q'' - \lambda Q + 2\kappa Q^3 - \varepsilon = 0, \qquad (2.48)$$

where the prime indicates the derivative with respect to *T*. Here the scaling variables are given by

$$T = \frac{\tau - \tau_c}{1 - c_0 R(z)}, \qquad \kappa = -\frac{\gamma(0)}{\beta(0)}. \qquad (2.49)$$

2.7 The rational solutions

Our goal in this section is to present the rational solutions of Eq. (2.48), following the results of the previous section. In the same manner we start with a fractional transform (FT) [34]

$$Q(T) = \frac{A + Bf^2(T,m)}{1 + Df^2(T,m)}, \qquad (2.50)$$

that connects the solutions of the damped NLSE with a source, to the elliptic equation $f'' \pm af \pm \lambda f^3 = 0$. As has been done previously, the coefficients of $f^n(T, m)$ for n=0,2,4,6 can be set to zero to reduce the problem to an algebraic one, and obtain the solutions. In getting the algebraic equations, use has been made of the following relations for various derivatives of f: $f'' = / + f^3$, and $f'^2 = \frac{1}{2}f^4 + 2E_0$, where E_0 is the integration constant. Furthermore, it is assumed that f can be taken as any of the three Jacobi elliptic functions with an appropriate modulus parameter: $\mathrm{cn}(T, m)$, dn(T, m), and $\mathrm{sn}(T, m)$. The other nonsingular solutions can be derived analogously. Various limiting conditions of cnoidal functions are: $\mathrm{cn}^2(T, 0) = \cos^2(T)$, and $\mathrm{cn}^2(T, 1) = \mathrm{sech}^2(T)$; $\mathrm{dn}^2(T, 0) = 1$, $\mathrm{cn}^2(T, 1) = \mathrm{sech}^2(T)$; $\mathrm{sn}^2(T, 0) = 0$, and $\mathrm{sn}^2(T, 1) = \tanh^2(T)$.

For definiteness, we start with the assumption $/ = \mathrm{cn}(\xi, m)$; evidently, the coefficients of $\mathrm{cn}^n(T, m)$, for $n = 0, 2, 4, 6$ can be set to zero, and thereby yielding four algebraic equations. The identities satisfied by the cnoidal functions make them amenable for finding the exact solutions of the nonlinear ODE of the form described by Eq. (2.48). In simplifying the second derivative of Q, we used the following important identities satisfied by the cnoidal functions.

$$\mathrm{cn}^2\mathrm{sn}^2\mathrm{dn}^2 = \mathrm{cn}^2(1 - m) + (2m - 1)\mathrm{cn}^4 - m\mathrm{cn}^6$$

$$\mathrm{cn}^4\mathrm{dn}^2 - m\mathrm{cn}^4\mathrm{sn}^2 = \mathrm{cn}^4(1 - 2m) + 2m\mathrm{cn}^6$$

$$\mathrm{cn}^2\mathrm{dn}^2 - \mathrm{sn}^2\mathrm{dn}^2 - m\mathrm{cn}^2\mathrm{sn}^2 = 2\mathrm{cn}^2(1 - 2m) + 3m\mathrm{cn}^4 + m - 1. \qquad (2.51)$$

The four consistency conditions are:

$$-\lambda A - 2(AD - B)(1 - m) + 2\kappa A^3 - \varepsilon = 0, \quad (2.52)$$

$$2\{AD - B\}\{3D - 3mD - 4m + 2) - 2X\{AD + B) + 6\kappa A^2 B - 3\varepsilon D = 0, \quad (2.53)$$

$$2\{AD - B)(3m + 4mD - 2D) - XD(AD + 2B) + 6\kappa AB^2 ... 3\varepsilon D^2 = 0, \quad (2.54)$$

$$-\lambda BD^2 - 2m(AD - B)D + 2\kappa B^3 - \varepsilon D^3 = 0. \quad (2.55)$$

In general, the rational solutions are unstable and may blow up. A number
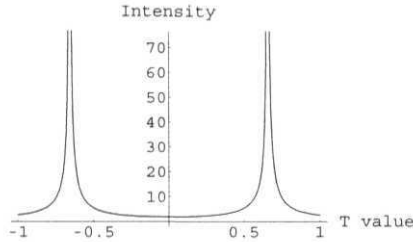
Figure 2.3: Plot depicting the singular solitary solution.

of rational solutions we have found are stable, as evidenced from the numerical stability. Thus, we shall present them here, with the specifications for the regimes in which they apply. Some of the periodic and hyperbolic solutions are presented below.

Case(I): Trigonometric solution

For $A = 0$; and $m = 0$; we find that

$$Q(T) = (\varepsilon/2)\frac{\cos^2(T)}{1 - (2/3)\cos^2(T)}. \tag{2.56}$$

Case(II): Hyperbolic solution

For $B = 0$, and $m — 1$; we find that

$$Q(T) = (3/4)\varepsilon\frac{1}{1 - (3/2)\text{sech}^2(T)}. \tag{2.57}$$

This is a singular solution. The singularity here corresponds to an extreme increase of the field amplitude due to self-focussing. If we consider the case, $AD = 1$, and $B = 0$; then we get a non-singular, hyperbolic solution

$$Q(T) = \frac{(\lambda - 8)}{6}\frac{1}{1 + D\text{sech}^2(T)}, \tag{2.58}$$

where $D = \frac{6}{(\lambda-8)}$, and $\lambda = \frac{16\pm\sqrt{256-4\alpha}}{2}$ with $\alpha = 18\varepsilon + 64$. To avoid the singularity, α should be always positive.

Case(III): Pure cnoidal solutions

(i) For $m = 5/8$; $A = 0$; it is found that, for the specific value of $A = 7/2$ we obtain a periodic cnoidal solution

$$Q(T) = (4/3)\varepsilon \frac{\mathrm{cn}^2(T, m)}{1 + \mathrm{cn}^2(T, m)}. \tag{2.59}$$

$$Q(T) = (4/3)\varepsilon \frac{\mathrm{cn}^2(T, m)}{1 - \frac{5}{9}\mathrm{cn}^2(T, m)}. \tag{2.60}$$

(iii) For $m — 1/2$; $A — 0$; it is found thai another specific value of $A = \pm 2\sqrt{3}$, yields yet another pure cnoidal solution

$$Q(T) = \varepsilon \frac{\mathrm{cn}^2(T, m)}{1 \pm \frac{1}{\sqrt{3}}\mathrm{cn}^2(T, m)}. \tag{2.61}$$

For the sake of clarity, all these solutions are tabulated below.

Table II. Various limits for the exact solutions of NLSE in an opaque medium with a source

Modulus parameter (m)	A	£	D	Rational solution $Q(T)$
0	0	**e/2**	-2/3	$\left(\frac{\varepsilon}{2}\right)\frac{\cos^2(T)}{1-\frac{2}{3}\cos^2(T)}$
1	$3\varepsilon/4$	0	-3/2	$\left(\frac{3\varepsilon}{4}\right)\frac{1}{1-\frac{3}{2}\mathrm{sech}^2(T)}$
5/8	0	$4\varepsilon/3$	1	$\left(\frac{4\varepsilon}{3}\right)\frac{\mathrm{cn}^2(T,m)}{1+\mathrm{cn}^2(T,m)}$
5/8	0	$4\varepsilon/3$	-5/9	$\left(\frac{4\varepsilon}{3}\right)\frac{\mathrm{cn}^2(T,m)}{1+\mathrm{cn}^2(T,m)}$
1/2	0		$\pm(1/\sqrt{3})$	$\varepsilon\frac{\mathrm{cn}^2(T,m)}{1\pm\frac{1}{\sqrt{3}}\mathrm{cn}^2(T,m)}$
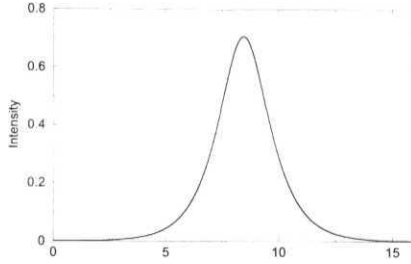
Figure 2.4: Plot depicting the stable solitary solution when the source is switched off. The parameter values are: $e - 0.0$, A $= 1.0$, and $\kappa = 5.0$.

Case(IV):

At this point it is worth mentioning that the following two cases are forbidden due to the fact that the source term is a vanishing one: For $m = 0$; $D - 0$ is forbidden and for $m = 1$; $A - 0$ is forbidden. In principle, one could have considered other cases also, but not all of them are interesting.

2.8   Numerical results

In this section we present the numerical corroborations of our analytical insights. We have solved Eq. (2.48) for various parameters values, using RK-4 method for a step size of $h = 10^{5}$. We find oscillatory solutions, as was anticipated from the analytical result (Case(I)). After switching off the source, we also identify localized soliton solution for the same parameter values, in order to compare with the results reported in Ref.[33]. The same have been depicted in figures 2.4-2.6.

This tecnique may find applications in pulse compression. Since this area is rather new, one needs to explore the full potential of this possibility in more detail.
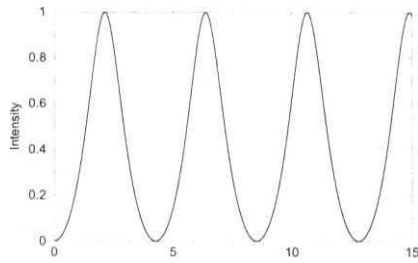
Figure 2.5: Plot depicting the oscillatory solution when the source is switched on. The parameter values are: $\varepsilon = 0.5$, A $= 1.0$, and $\kappa = 5.0$.
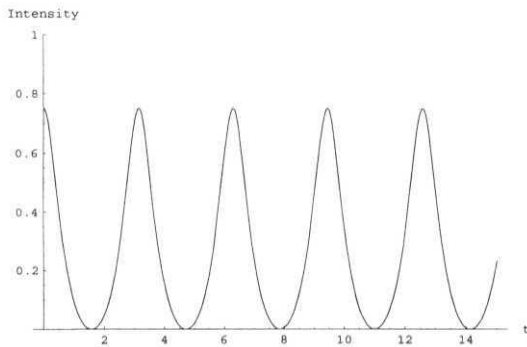
Figure 2.6: Plot depicting the oscillatory solution of Eq. (2.56) for same parameter values as above.

References

[1] N. Yajima, M. Oikawa, J. Satsuma, and C. Namba, Rep. Res. Appl. Mech. **XXII,** No. 70 (1975).

[2] A. Hasegawa, *Optical Solitons in Fibers* (Springer-Verlag, New York, 1990).

[3] V.E. Zakharov and A.B. Shabat, Sov. Phys. JETP 34, 62 (1972).

[4] A. Scott, *Nonlinear Science: emergence and dynamics of coherent structures* (Oxford University Press, Oxford, 1999).

[5] D.J. Kaup and A.C. Newell, Proc. R. Soc. London, Ser. A **361,** 413 (1978).

[6] A.W. Snyder and J.D. Love, *Optical Waveguide Theory* (Chapman and Hall, London, 1983).

[7] B.A. Malomed, Phys. Rev. E 51, R864 (1995).

[8] G. Cohen, Phys. Rev. E **61,** 874 (2000).

[9] P.S. Lomdahl and M.R. Samuelsen, Phys. Rev. A 34, 664 (1986).

[10] D.J. Kaup and A.C. Newell, Phys. Rev. B 18, 5162 (1978).

[11] K. Nozaki and N. Bekki, Physica D 21, 381 (1986).

[12] L. Friedland, Phys. Rev. E 58, 3865 (1998).

[13] I.V. Barashenkov, Yu.S. Smirnov, and N.V. Alexeeva, Phys. Rev. E 57, 2350 (1998).

[14] I.V. Barashenkov, E.V. Zemlyanaya, and M. Bar, Phys. Rev. E 64, 016603 (2001).

[15] H.E. Nistazakis, P.G. Kevrekidis, B.A. Malomed, D.J. Frantzeskakis, and A.R. Bishop Phys. Rev. E 66, R015601 (2002).

[16] G.P. Agrawal, *Nonlinear Fiber optics* (Academic Press, Boston, 1989).

[17] G.B. Whitham, *Linear and Nonlinear Waves* (Wiley, New York, 1974).

[18] S.P. Novikov, S.V. Manakov, L.P. Pitaevskii, and V.E. Zakharov, *Theory of Solitons. The Inverse Scattering Method* (Consultants Bureau, New York, 1984) and references therein.

[19] M. Abramowitz and A. Stegun, *Handbook of Mathematical Functions* (Dover Publications, New York, 1970).

[20] P.G. Drazin and R.S. Johnson, *Solitons: An introduction* (Cambridge University Press, Cambridge, 1989).

[21] A. Das, *Integrable Models* (World Scientific, Singapore, 1989).

[22] R.M. Miura, J. Math. Phys. 9, 1202 (1968).

[23] W.H. Press, B.P. Flannery, S.A. Teukolsky, and W.T. Vellerling, *Numerical Recipes in Fortran* (Cambridge University Press, Cambridge, 1992).

[24] J.C. Eilbeck, P.S. Lomdahl, and A.C. Newell, Phys. Lett. A 87, 1 (1981).

[25] G. Wysin and A.R. Bishop, J. Magn. Magn. Mater. 54-57 (1986) 1132.

[26] A.M. Kosevich, B.A. Ivanov, and A. S. Kovalev, Phys. Rep. **194,** 118 (1990).

[27] K. Nozaki and N. Bekki, Phys. Rev. Lett. 50, 1226 (1983); Phys. Lett. A **10, 383** (1984); J. Phys. Soc. Jpn. 54, 2363 (1985).

[28] A. Hasegawa and Y. Kodama, *Solitons in Optical Communications* (Oxford University Press, Oxford, 1995).

[29] M.J. Ablowitz and Z.H. Musslimani, Phys. Rev. E 67, 025601(R) (2003).

[30] T. Okamawari, A. Maruta, and Y. Kodama, Opt. Lett. **23,** 694 (1998).

[31] R. Driben and B.A. Malomed, Phys. Lett. A **301,** 19 (2002).

[32] J.D. Moores, Opt. Lett. **21,** 555 (1996).

[33] V.I. Kruglov, A.C. Peacock, and J.D. Harvey, Phys. Rev. Lett. **90,** 113902 (2003).

[34] T. Soloman Raju, C. Nagaraja Kumar, and P.K. Panigrahi, nlin.SI/0308012, submitted to Phys. Rev. Lett.

Chapter 3

Compactons

3.1 Introduction

Compactons are a new class of localized solutions of families of fully non-linear, dispersive, partial differential equations. Unlike the solitons, which, although highly localized, still have infinite span, these solutions have compact support; they vanish identically outside a finite region. Hence, these solitary waves have been christened as compactons [1]. There is strong numerical support that, the collision of two compactons is elastic, a feature characteristic of the solitons. The aforementioned nonlinear equations, arising in the context of pattern formation in nonlinear media, seem to have only a finite number local conservation laws; yet the behavior of the solutions closely mimic those of the solitons of the integrable models.

The first two parameter family of fully nonlinear, dispersive, equations admitting compacton solutions, are of the form,

$$u_t + (u^m)_x + (u^n)_{3x} = 0 \qquad (3.1)$$

for $m > 0$, $1 < n < 3$. These equations arose in the process of understanding the role of nonlinear dispersion in the formation of structures like liquid

drop models [2]. The compacton solution of $K(2,2)$ for example reads

$$u_c = \frac{4\lambda}{3}\cos^2(\frac{x - \lambda t}{4}) \; , \qquad (3.2)$$

when $|\, x - \lambda t \,| < 2n$ and $u_c = 0$, otherwise.

Unlike the solitons, the width here is independent of velocity; however, the amplitude depends on it. It has been shown that, $K(2,2)$ admits only four local conservation laws. Some of the other representative compactons, in appropriate ranges are,

$$u_c = [375A - (x - \lambda t)^2]/30 \quad , \qquad (3.3)$$

and

$$u_c = \pm\sqrt{[3\lambda/2]}cos((x - \lambda t)/3) \quad ; \qquad (3.4)$$

these are the solutions of A'(3,2), and A'(3,3) equations, respectively. The $K(m,n)$ family is not derivable from a first order Lagrangian, except for $n = 1$ [3]. A generalized sequence of KdV-like equations, which could be given a Lagrangian formulation, have also been shown to admit compacton solutions. These equations

$$u_t + u_x u^{l-2} + \alpha[2u_{3x}u^p + 4pu^{p-1}u_x u_{2x} + p(p - 1)u^{p-2}(u_x)^3] = 0, \qquad (3.5)$$

have the same terms as in Eq. (3.1); the relative weights of the terms are different. Further generalizations to, one parameter generalized KdV equation [4], two parameter odd order KdV equations [5], enlarged the class of evolution equations, which admitted solutions with compact support. These type of solutions have also appeared in the context of baby Skyrmions [6]. The stability of the compacton solutions was considered in Ref. [7]; it was shown, by linear stability analysis, as well as, by Lyapunov stability criterion, that, these solutions are stable for arbitrary values of the nonlinear parameters.

It should be noted that, KP and Boussinesq equations have been suitably modified in order that they support compacton solutions [9]. In light

of this, it is of great interest to probe the existence of compacton solutions for other known integrable nonlinear equations like modified KdV (MKdV) and NLSE, or the generalizations thereof. In particular, one would like to compare their properties with the soliton solutions of these equations. Furthermore, the possibility of these compact solutions arising from the nonlinear equations, relevant for physical problems, will make them amenable for experimental detection. Akin to the compacton bearing equations mentioned above, a number of these integrable hierarchy of equations also arose from anharmonic chains and are also relevant to plasma physics.

As is clear from the above analysis, one needs to first find the periodic solutions of the nonlinear equations, before compactifying them in a suitable interval. in what follows we will concentrate on MKdV and NLSE equations, whose periodic solutions are well studied [8]. We will make use of special periodic solutions of the rational type, which are not well illustrated in the literature. Hence, we use the same procedure, as employed in the earlier chapter, to first obtain the rational periodic solutions of the above equations. It should be noted that, KP and Boussinesq equations have been suitably modified in order that they support compacton solutions [9]. It will be shown here that, one needs to append appropriate source terms to MKdV and NLSE equations for obtaining compacton solutions.

We first present the newly found rational solutions of MKdV equation. It is worth mentioning that, the MKdV equation [10] is connected with the KdV equation via the Miura transformation [11]. It finds applications in various branches of science. Zabusky had shown how this equation may model the oscillations of a lattice of particles connected by nonlinear springs, as the Fermi-Pasta-Ulam model does [12]. Apart from the solitary wave solutions, breather solutions are also known for MKdV equation [13]. Below we first present the rational solutions, which contain both trigono-

metric and hyperbolic solutions. Although, we present the modification
of the MKdV which can give rise to compacton solutions; it was found
numerically that the trigonometric solutions are not stable under MKdV
evolution.

3.2 Some rational solutions of MKdV equation

The MKdV equation reads as

$$u_t + u^2 u_x + u_{3x} = 0, \tag{3.6}$$

where $u = u(x,t)$ and a subscript denotes partial **differentiation**,*e.g.*, $u_x = \frac{\partial u}{\partial x}$, and u_{3x} - $\frac{\partial^3 u}{\partial x^3}$. By introducing the traveling wave assumption

$$z - \gamma\alpha(x - vt)$$

one gets the ordinary differential equation

$$-v\gamma\alpha u_z 4 - \gamma\alpha u^2 u_z + \gamma^3\alpha^3 u_{3z} = 0. \tag{3.7}$$

We start with a solution of Eq. (3.6):

$$z) = \frac{A \ 4 \ B\gamma^2 \text{cn}^2(z,m)}{1 + D\gamma^2 \text{cn}^2(z,m)},$$

Setting $7 = 1$, for the sake of convenience, the three algebraic equations
are:

$$-v + A^2 - 12D\alpha^2 + 12mD\alpha^2 + 8m\alpha^2 - 4a^2 = 0, \tag{3.8}$$

$$-Dv4 \ 6AB - 16mD\alpha^2 + 8D\alpha^2 + 6D^2\alpha^2 - 6mD^2\alpha^2 - 6m\alpha^2 = 0, \tag{3.9}$$

$$-D^2v + B^2 + 12mD\alpha^2 \ i \ 8mD^2\alpha^2 - 4D^2\alpha^2 = 0. \tag{3.10}$$

We shall present the five, *rational solutions* with the specifications for
the regimes in which they apply. The five solutions, numbered Case(i)

to Case(iv), are presented in the order that appears to be most natural; Case(i) corresponds to trigonometric regime, **Case(ii)** and Case(iii) correspond to hyperbolic regime, and Case(iv) and Case(v) correspond to pure cnoidal solutions with a modulus parameter m. Case(i):

For $A = 0$, $m = 0$; we found that $v = 4a^2$. Then we arrive at the periodic solution,

$$u(z) = \alpha\left(\frac{4\sqrt{2}}{3}\right)\frac{\cos^2(z)}{1 - \frac{2}{3}\cos^2(z)}. \tag{3.11}$$

Case(ii):

For A - 0, $m = $ J; we found that $v = 1\alpha^2$. This yields, the hyperbolic solution,

$$u(z) = \sqrt{6}\alpha\frac{\operatorname{sech}^2(z)}{1 - \frac{1}{2}\operatorname{sech}^2(z)}. \tag{3.12}$$

Case(iii):

For $B = 0$, $m = 1$; we found that $v = -4a^2$. This results in another

$$u(z) = \sqrt{-8}\alpha\frac{1}{1 - \frac{3}{2}\operatorname{sech}^2(z)} \tag{3.13}$$

Case(iv):

For $A = 0$, $D - 1$, and $m = 5/8$; we found that $v = -\frac{7}{2}\alpha^2$. This gives rise to the cnoidal solution,

$$a(z) = 2\sqrt{-3}\alpha\frac{\operatorname{cn}^2(z,m)}{1 + \operatorname{cn}^2(z,m)}. \tag{3.14}$$

Case(v):

For $A = 0$ and $m = 1/2$; it is found that $v = -2\sqrt{3}\alpha^2$. This results in another cnoidal solution:

$$a(z) = \alpha\left(\sqrt{-8/\sqrt{3}}\right)\frac{\operatorname{cn}^2(\xi,m)}{1 + \frac{1}{\sqrt{3}}\operatorname{cn}^2(\xi,m)}. \tag{3.15}$$

Table I. Various limits for the exact solutions of MKdV

Modulus parameter (m)	A	B	D	$u(\xi)$
0	0	$\alpha\frac{4\sqrt{2}}{3}$	$-2/3$	$\alpha\frac{4\sqrt{2}}{3}\frac{\cos^2(\xi)}{1-\frac{2}{3}\cos^2(\xi)}$
1	0	$\sqrt{6}\alpha$	$-1/2$	$\sqrt{6}\alpha\frac{\mathrm{sech}^2(\xi)}{1-\frac{1}{2}\mathrm{sech}^2(\xi)}$
1	$\sqrt{-8\alpha}$	0	$-3/2$	$\sqrt{-8\alpha}\frac{1}{1-\frac{3}{2}\mathrm{sech}^2(\xi)}$
$\frac{5}{8}$	0	$\alpha 2\sqrt{-3}$	1	$\alpha 2\sqrt{-3}\frac{\mathrm{cn}^2(\xi,m)}{1+\mathrm{cn}^2(\xi,m)}$
$1/2$	0	$\alpha\sqrt{\frac{-8}{\sqrt{3}}}$	$1/\sqrt{3}$	$\alpha\sqrt{\frac{-8}{\sqrt{3}}}\frac{\mathrm{cn}^2(\xi,m)}{1+\frac{1}{\sqrt{3}}\mathrm{cn}^2(\xi,m)}$

3.2.1 Numerical results

In this section we present the numerical stability of the exact periodic solution of MKdV. This is accomplished by discretizing the space and time variables by a centered finite-difference scheme as

$$\frac{\partial u}{\partial t} = \frac{u(i,j+1)-u(i,j-1)}{2\triangle t}, \qquad (3.16)$$

$$\frac{\partial u}{\partial x} = \frac{u(i+1,j)-u(i-1,j)}{2\triangle x}, \qquad (3.17)$$

and the third derivative is descretized as

$$\frac{\partial^3 u}{\partial x^3} = \frac{u(i+2,j)+2u(i-1,j)-2u(i+1,j)-u(i-2,j)}{\triangle x^3}. \qquad (3.18)$$

If we plug all these relations into Eq. (3.6), we obtain the recurrence
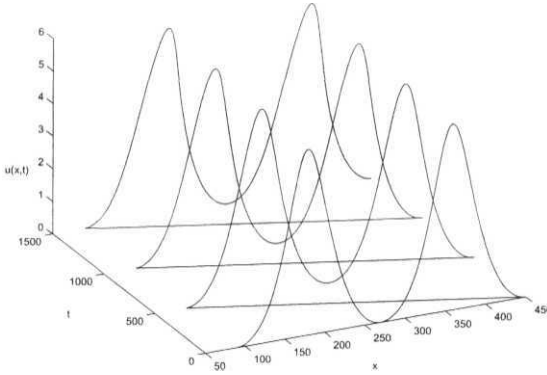
Figure 3.1: Plot depicting the evolution of the periodic solution, under MKdV.

relations

$$u(i, j+1) \simeq u(i, j-1) - \frac{\Delta t}{3\Delta x}[u(i+1,j) + u(i,j) +$$
$$u(i-1,j)]^2[u(i+1,j) - u(i-1,j)] - \frac{\Delta t}{\Delta x^3}[u(i+2,j) +$$
$$2u(i-1,j) - 2u(i+1,j) - u(i-2,j)]. \qquad (3.19)$$

Here, the factor u^2 is taken as the average of the three values centered at *(i,j)* in a row. The initial conditions chosen from the exact solution are knitted on a lattice, with appropriate grid size. For the grid size $dx = 0.95$, and $dt = 0.004$, after some evolution the onset of instability is seen. The same has been depicted in the accompanying two figures Figs. 3.1, 3.2.
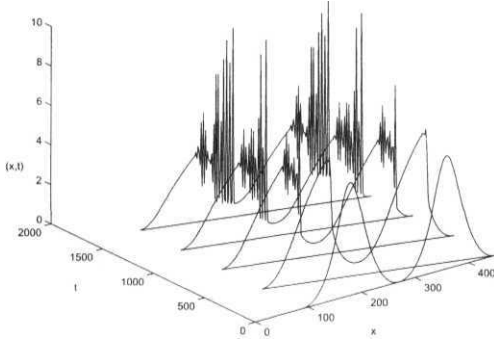
Figure 3.2: Plot depicting the onset of instability in the periodic solution.

3.3 Periodic rational solutions of Boussinesq equation

In this section we present the rational solutions of the Boussinesq equation (BE) [14], which describes the motion of the long water waves moving in both the directions. Unlike KdV equation, the solitary waves of the BE, during collision behave differently. The wave with smaller amplitude take over the wave with larger amplitude.

We use the same fractional transformation to find the solutions of BE, which was used in the case of NLSE with a source, and MKdV. Recently, the continuous spectrum and the soliton solutions for the BE have been investigated using the $\bar{\partial}$-method [15]. The BE reads

$$u_{tt} - u_{xx} - 6u_{xx}^2 - u_{4x} = 0, \qquad (3.20)$$

In order to obtain the moving solutions, we introduce $z = \alpha(x - vt)$. The BE will take ODE form

$$\epsilon u'' - 6(u^2)'' - \alpha^2 u'''' = 0 \qquad (3.21)$$

where e = v^2 - 1. By the fractional transformation used earlier, we obtain the consistency conditions from which we could find a rational solution. We have found that only for $m = 0$, there exists a solution. The consistency conditions for m=0, are

$$-2\epsilon + 24A \quad 24\alpha^2 D + 24\alpha^2 D^2 - 8a^2 = 0$$

$$6\epsilon D^2 + 48BD^2 - 160\alpha^2 D^3 = 0$$

$$2e.D'^2 - 48BD - 72BD^2 + 96AD^2 + 56\alpha^2 D^2 + 384\alpha^2 D^3 = 0$$

$$10\epsilon D^2 + 4\epsilon D - 72B + ASAD - 120AD^2 - 176\alpha^2 D$$

$$+320\alpha^2 D^2 - 216\alpha^2 D^3 = 0$$

$$4\epsilon + 2\epsilon D + 48B - 48A - 96AD + 200\alpha^2 D + 48\alpha^2 D^2$$

$$-24\alpha^2 D^3 - 16a^2 = 0. \tag{3.22}$$

For $A = 0$; we found a trigonometric solution given by

$$u(z) = B\frac{\cos^2(z)}{1 + D\cos^2(z)}, \tag{3.23}$$

where $B = (5/3)[-b+\sqrt{b^2-4c}] - (\varepsilon/8)$, and $D = \frac{-b\pm\sqrt{b^2-4c}}{2}$, with $b = 9\epsilon/146\alpha^2 - 104/146$, and $c = 24f/146a^2$.

3.4 Compactons of MKdV equation with a source

As seen earlier, a periodic solution to the MKdV equation,

$$u_t + u^2 u_x + u_{3x} = 0 \quad , \tag{3.24}$$

which is well defined and a traveling wave solution is of the form,

$$u_p(x,t) = \frac{\sqrt{32}}{3}k\frac{\cos^2 k(x - 4k^2 t)}{(1 - \frac{2}{3}\cos^2 k(x - 4k^2 t))} . \tag{3.25}$$

One immediately notices that, the MKdV equation supports a compacton solution,

$$u_c(\xi) = \frac{\sqrt{32}}{3}k\frac{\cos^2 k(\xi)}{(1 - \frac{2}{3}\cos^2 k(\xi))}\Theta, \tag{3.26}$$

with

$$\Theta \equiv [\theta(\xi + \frac{\pi}{2k}) - \theta(\xi - \frac{\pi}{2k})] \quad ,$$

and

$$\xi = x - 4k^2 t \quad ,$$

if a source term of the type,

$$\Pi = 2\frac{\sqrt{32}}{3}k^3[\delta(\xi - \frac{\pi}{2k}) - \delta(\xi + \frac{\pi}{2k})],$$

is included. Note that, for this compact solution, both the width and amplitude are proportional to the square root of the velocity. This behaviour is reminiscent of the solitons. It should be further noticed that, the strength of the moving point sources, determine the velocity of the compacton. At this point, one needs to be careful with the conserved quantities, in light of the fact that some derivatives of the solution are discontinuous at the boundaries. The Hamiltonian from which the MKdV equation with a source term, can be derived by variational principle,

$$H = \frac{1}{2} \int_{-\infty}^{\infty} u_x^2 dx - \frac{1}{12} \int_{-\infty}^{\infty} u^4 dx + \int_{-\infty}^{\infty} u\Pi dx \quad , \tag{3.27}$$

and the momentum expression, given by,

$$P = \frac{1}{2} \int_{-\infty}^{\infty} u^2 dx \quad , \tag{3.28}$$

are well defined at the edges. Explicitly, for the above solution, the energy and momentum are given, respectively by, $E_c = - (16/3)\pi A^3 + 2.07\pi$ and $P_c = -4 \pi k$. For the soliton solution of the MKdV equation

$$u_s(x,t) = \sqrt{6}k\mathrm{sech}k(x - k^2 t) \tag{3.29}$$

the corresponding quantities are $E_s = -2 k^3$ and $P_s - 6 k$. Other conserved quantities involving the even derivatives of the solutions, are not well defined at the boundaries. In this sense, these solutions are similar to compactons of the non-integrable models.

3.5 Compactons of NLSE with source

Below, we show that the above compacton solution of MKdV is also a strong solution of the NLSE, and higher order KdV-like equations, with appropriate sources. We start with the NLSE with a source:

$$i\partial_t q + \frac{\hbar^2}{2}\partial_x^2 q + |q|^2 q - \eta = 0 \quad . \tag{3.30}$$

Using the following ansatz,

$$q(x,t) = e^{[\psi(\xi')-\omega t]}a(\xi'), \tag{3.31}$$

where $\xi' = x - vt$, and choosing the source term as $\eta(\xi') = k\bar{\Pi}e^{[\psi(\xi')-\omega t]}$, we can separate the real and the imaginary parts of the equation as,

$$v\psi' + \omega a + \frac{a''}{2} - \frac{\psi''}{2}a + a^3 - k\bar{\Pi} = 0, \tag{3.32}$$

and

$$va' + \frac{\psi''}{2}a + \psi'a' = 0. \tag{3.33}$$

Equation (3.33) can be straightforwardly solved to give

$$\psi' = v + \frac{P}{a^2},$$

where P is the integration constant. Choosing $P - 0$, we arrive at the compacton:

$$a(\xi') = (\frac{16k}{27})^{1/3}\frac{\cos^2[(\frac{27}{16})^{\frac{1}{6}}k^{\frac{1}{3}}\xi]}{1 - \frac{2}{3}\cos^2[(\frac{27}{16})^{\frac{1}{6}}k^{\frac{1}{3}}\xi]}\bar{\Pi}, \tag{3.34}$$

where ft $= [\theta(\xi' + \frac{\pi}{2}) - \theta(\xi' - \frac{\pi}{2})]$.

We now show that the above periodic solution also satisfies higher order, one parameter dependent, KdV-like equations:

$$u_t + (lu + mu^4)u_x + 5u^2u_{3x} + pu_{5x} = 0 \quad , \tag{3.35}$$

Explicitly, the solution of this equation is given by,

$$u_p(x,t) = \frac{4}{3}\frac{\cos^2 k(x - 4k^2t)}{(1 - \frac{2}{3}\cos^2 k(x - 4k^2t))} \tag{3.36}$$

where $l = \frac{10}{3p}$, $rn = \frac{5}{3p}$ and $k^2 = \frac{1}{4p}$. Note that, for this solution the amplitude is independent of the velocity, where as the width depends on it. Interestingly, the following fifth order KdV-like equation,

$$u_t + lu^4 u_x + u_x^3 + u^2 u_{3x} + qu_{5x} = 0, \tag{3.37}$$

has a periodic solution of the similar form:

$$u_p(x,t) = \frac{2\sqrt{10}}{3} \frac{\cos^2 k(x - 4k^2 t)}{(1 - \frac{2}{3}\cos^2 k(x - 4k^2 t))}, \tag{3.38}$$

for $/ = '-$ and $k^2 = \div$. These solutions can be provided a compact support by adding appropriate source terms in their respective nonlinear equations.

References

[1] P. Rosenau and J.M. Hyman, Phys. Rev. Lett. 70, 564 (1993).

[2] F. Cooper, H. Shepard, and P. Sodano, Phys. Rev. E 48, 4027 (1987).

[3] A. Khare and F. Cooper, Phys. Rev. E 48, 4853 (1998).

[4] B. Dey, Phys. Rev. E **57,** 4733 (1998).

[5] T. Gisiger and M.B. Paranjape, Phys. Rev. D **55,** 7731 (1997).

[6] B. Dey and A. Khare, Phys. Rev. E 58, 2741(R) (1998).

[7] A. Das, *Integrable Models,* (World Scientific, Singapore, 1989).

[8] S.P. Novikov, S.V. Manakov, L.P. Pitaevsky, and V.E. Zakharov, Theory of Solitons: The Inverse Scattering Method (Consultants Bureau, New York, 1984).

[9] P. Rosenau, Phys. Lett. A **275,** 193 (2000).

[10] M. Wadati, J. Phys. Soc. Jpn. 32, 1681 (1972); 34, 1289 (1973)

[11] R.M. Miura, J. Math. Phys. 9 1202 (1968).

[12] N.J. Zabusky, *A synergetic approach to problems of nonlinear dispersive wave propagation and interaction. In nonlinear partial differential equations,* ed. W. F. Ames, 223-58, Academic Press, Newyork (1967).

[13] P.G. Drazin, *Solitons* , London Mathematical Society Lecture Notes Series, 85 (Cambridge University Press, New York, 1983).

[14] J. Boussinesq, J. Math. Pures. Appl. 7, 55 (1872).

[15] L.V. Bogdanov and V.E. Zakharov, Physica D **165,** 137 (2002).

[16] A. Oran and P. Rosenau, Phys. Rev. A 39, 2063 (1989).

Chapter 4

Two-species Bose-Einstein Condensate

4.1 Introduction

In this chapter we describe the utility of the NLSE, which is known to be GP equation, in aptly describing the dynamics of the Bose-Einstein condensate (BEC) as a mean field theoretic approximation. First we describe briefly the single component BEC, by deriving various interesting properties of the condensates. Then we explore some interesting physical features of TBEC. We also present the numerical simulations whenever, the GP equation is intractable for the analytical methods, for various coupling strengths. However, we have obtained exact solutions for various parameter values of the low density limit.

The phenomenon of trapped bosons (mainly alkali atoms like H, Li, Na, Rb) undergoing BEC has been the subject of intense research in recent times. The dynamics of the condensed phase is effectively captured by the GP equation which has a cubic nonlinearity, originating from the effective point-interaction of the trapped atoms at ultra-cold temperatures. The fact that these type of nonlinear equations are ubiquitous in nonlinear optical systems allows one to borrow many results from the same and apply it

to BEC. Elongated BEC has also been realized in quasi-one dimensional regime, under a weaker longitudinal confinement. This quasi-one dimensional cylindrical BEC has been extensively studied, particularly for the possibility of observing solitary wave solutions. A number of experiments have observed dark solitons, in case of repulsive interactions. This has also led to the possibility of observing the Lieb mode as compared to the Bogoliubov modes, which are analogous to sound modes in elastic media. The use of the Feshbach resonance on these systems has led to the possibility of tuning the interaction strength from repulsive to attractive, with desired strength. Recently, solitons and soli ton trains have been seen in the attractive BEC. Although the presence of traps is necessary to stabilize the BEC in higher dimensions; the delicate balance of the nonlinearity and the dispersion can produce stable localized structures in quasi-1D geometry. Recently such solitons and soli ton trains have been observed in the single component BEC of ^{7}Li. The soliton trains particularly show interesting behavior. In the weakly attractive regime, the pulse trains have been observed with the neighboring ones having a phase difference of π. The mechanism of production of these type of nonlinear waves has also received considerable attention in recent times, since the known procedures like the modulation instability have been found to be inadequate.

TBEC have been recently produced and have been studied in both quasi-1D and higher dimensions. Although soliton solutions have been studied quite extensively, using the connection of the GP equation with the Manakov system [1], the solitary train solutions have not been investigated in detail. Hence, a good part of this chapter attempts to analyze exhaustively the solitary wave solutions of the TBEC in the quasi-1D, in particular the low density regime, and strong coupling limit. The former is studied analytically, whereas the latter is studied numerically.

4.2   Bose-Einstein condensation

Christened in the name of its discoverer, Albert Einstein in 1925, BEC is a paradigm of quantum statistical phase transitions. It occurs when the mean particle separation is comparable with the de Broglie wavelength and is manifested by an abrupt growth in the population of the ground state of the potential confining the Bose gas. Thus, the experimental realization of BEC requires creating a sample of Bosonic particles at extremely low temperatures and high densities was a long standing problem. Finally in 1995, the physicists from JILA and MIT, created BEC in ^{87}Rb, and ^{23}Na, by combining the laser cooling and evaporative cooling techniques.

Consider an ideal Bose gas consisting of N noninteracting particles of mass m, contained in a box of volume V, characterized by the de Broglie wavelength $\lambda_{dB} = (2\pi^2\hbar^2/m\kappa_B T)^{1/2}$, where T is the temperature and κ_B is the Boltzmann constant. For $\lambda_{dB} \ll d$, where d is the mean inter particle separation; the quantum effects are negligible and the particles behave classically. At high temperatures, therefore the momenta *(p)* of the particles are distributed according to the classical Maxwell-Boltzmann distribution. For low temperatures, λ_{dB} begins to approach d and the quantum effects become evident. At critical T, $\lambda_{dB} - d$. In the case of Bosons, since there is no restriction on the number of particles that can stay in any state, the quantum behavior is manifested by an increase in the occupation of states at small *p*. As the temperature is lowered further to zero, the quantum effects are dominant, and a macroscopic quantum state is formed with $p = 0$. This is referred to as *Bose-Einstein condensation.*

4.3   Single-component BEC

To describe the dynamics of the weakly interacting BEC, the GP equation [2] has been shown to be an appropriate theoretical frame work [3, 4, 5, 6,

7, 8, 9, 10]. At zero temperature this equation can be written as

$$i\hbar \frac{\partial \psi}{\partial t} = [-\frac{\hbar^2}{2m}\nabla^2 + V + U_0 \mid \psi^2 \mid]\psi, \tag{4.1}$$

where U_0 = *fofra/rn,* is the effective atom-atom interaction term. For $a < 0$, a bright soliton will emerge as the solution, while for the case $a > 0$, a dark soliton is a solution. Dark solitons in cigar-shaped BEC of RB[87] were created by phase imprinting method [11]. Also, the NIST group has investigated soliton like states in nearly spherical BEC's in Na[23] [12]. And, bright solitons were reported in BEC of Lithium atoms [13]. However, the GP equation could not be applied to describe BEC in liquid He[4], because of the large interaction and depletion.

Below, we study the GP equation to describe some interesting properties of single component BEC, following the derivation given in Refs. [14, 15, 16]. We study in detail, both the low density limit as well as high density limit using TF approximation. We also present the exact periodic solutions in attractive case.

We assume that a Bose-Einstein condensed atoms are confined in a cylindrical harmonic potential $V - m\omega_\perp^2(x^2 + y^2)/2$, and the wave motion is along z axis. There is no confinement along z axis. Further, we assume that the transverse dimension of the cloud is sufficiently small, such that the problem is reduced to a one dimensional one, and the solitary pulse can be described by a local velocity, $v(z)$, and a local density of particles per unit length, $\sigma(z)$, $\sigma(z) = \int' dxdy \setminus \Psi(x, y, z)|^2$. Thus, the wavefunction can be written as $\Psi(r, t) = f(z, t)g(x, y, \sigma)$,where g is the equilibrium wavefunction for the transverse motion which depends on time implicitly through the time dependence of σ. Choosing g to be normalized as $\int |g|^2 dxdy = 1$, and thus from the above equations, $|f|^2 = \sigma$.

Weak coupling limit: In this limit one can neglect the nonlinear term and solve the Schrodinger equation. This results in $|g|^2 = (\pi a_\perp^2)^{-1}e^{(-\rho/a}a^2$ and

noticing that $a\pm = (\hbar/m\omega_\perp)^{1/2}$. Thus the equation for / can be written as

$$i\hbar\partial_t f = -\frac{\hbar^2}{2m}\partial^2{}_x f + \hbar\omega_\perp(1 + 2a_{sc} \mid f \mid^2)f. \qquad (4.2)$$

By applying one more transformation

$$w = fe^{i\omega_\perp(1+2a\sigma_0)t}, \qquad (4.3)$$

$$i\hbar\partial_t w = -\frac{\hbar^2}{2m}\partial^2_x w + \hbar\omega_\perp 2a(\mid w \mid^2 -\sigma_0)w, \qquad (4.4)$$

where a is the scattering length, and the chemical potential is $\mu = \sigma_0\hbar\omega_\perp 2a$. By writing $w = \sqrt{\sigma}e^{i(\phi+\omega t)}$, we can separate the real and imaginary parts of Eq. (4.4) and obtain

$$v = u + \frac{c}{\sigma}, \qquad (4.5)$$

where c is the integration constant, and

$$2\sigma\sigma'' - \sigma'^2 + \Gamma\sigma^2 + g\sigma^3 - \delta = 0, \qquad (4.6)$$

where the effective 1D coupling $\hbar\omega_\perp a$ has been taken to be weakly attractive; $g = -16m\omega_\perp|a|/\hbar\Gamma = 4m^2u^2/\hbar^2 - 8m\omega/\hbar + 4\mu m/\hbar^2$, **and** $S = 4m^2c^2/\hbar^2$. **Furthermore,** we have assumed that both σ, and ϕ are functions of $(z - ut)$. In arriving at Eq. (4.6), use was made of the superfluid velocity $v = (\hbar/m)\partial_z\phi$

One finds both chirped and non-chirped solutions of the above equation. These are in the form of elliptic functions. The repulsive and attractive cases show distinct behavior for certain values of the modulus parameter $\tilde{m}$. Particularly in the repulsive case, for the soliton solution, the Lieb mode has been reported [16]. For the attractive case, the solution can be written as

$$\sigma = A + B\mathrm{cn}^2(z/\alpha\tilde{m}). \qquad (4.7)$$

In the limit $m = 1$, we find that $B = 8/g\alpha^2$, and $A = -(8/\alpha^2 + 2\Gamma)/3g$.
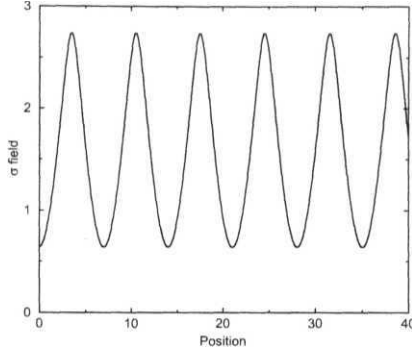
Figure 4.1: Plot depicting the amplitude of single component BEC (attractive case) for $u = 0.8$, $g = 1.0$, and $\mu = 0.2$.

Strong coupling limit:

For large nonlinearities U_0, we use TF approximation. Then it is observed that for the harmonic trap, the population density goes to zero at $r = \pm 2/\alpha\sqrt{\mu}$, where $\alpha^2 = 2m\omega_\perp$. Consequently, the normalization condition

$$\int |g|^2 \, dxdy = 1, \tag{4.8}$$

implies that $\mu - 4\hbar\omega_\perp a^{1/2}|f|$. In light of these results we can show that

$$i\hbar\partial_t f = -\frac{\hbar}{2m}\partial^2_z f + (2\hbar\omega_\perp 2a^{1/2} \mid f \mid)f. \tag{4.9}$$

By applying another transformation $/ = we^{2i\omega_\perp\sigma_0 t}$, we obtain the GP equation for strong coupling case

$$i\hbar\partial_t w = -\frac{\hbar^2}{2m}\partial^2_x w + \hbar\omega_\perp 2a(\mid w \mid - \mid w_0 \mid)w.$$

We again write $w = \sqrt{\sigma}e^{(i\phi+w)}$, and separate the real and imaginary parts. The real part is given by

$$\frac{d^2\sigma}{dz^2} = \frac{1}{2\sigma}\left(\frac{d\sigma}{dz}\right)^2 + \frac{2m^2c^2}{\hbar^2\sigma} - \frac{2m^2u^2}{\hbar^2}\sigma - g\sigma^{3/2} + g\sigma\sigma_0^{1/2} + \frac{4m\omega}{\hbar}\sigma. \tag{4.11}$$

This equation is solved numerically for the attractive case. The same has been depicted in Fig 4.1.

4.4   Two-component BEC

We study the solitary waves of TBEC in a quasi-1D geometry in particular, the soliton trains are investigated in detail, in light of their recent observation in one-component BEC. We study repulsive and attractive nonlinearities, both in the weak and strong coupling regimes, analytically and numerically. Chirped and nonchirped soliton trains, respectively, with or without a constant background are obtainbed analytically for the weak coupling case. A number of interesting features of the periodic and localized solutions are observed. In the attractive strong coupling case, for certain parameter values, we find that one of the species shows *autocorrelation traces* due to modulational instability, akin to a two laser system (Nd:YAG, and InGaAsP).

Much theoretical work has already gone into studying the ground state solutions of the coupled GP equations describing multi-component BECs [17, 18]. TBEC has been observed experimentally [19], where the two hyperfine levels of the [87]Rb act as the two components. In this case, a fortuitous coincidence in the triplet and singlet scattering lengths has led to the suppression of exoergic spin-exchange collisions, which lead to heating and resultant loss of atoms. A number of interesting features, like the preservation of the total density profile and coherence for a charc - teristically long time, in the face of the phase-diffusing couplings to the enviornment and the complex relative motions, point to the extremely interesting dynamics of the TBEC. The effects of spatial inhomogeneity, three-dimensional geometry, and dissipation are examined, in light of the dark-bright solitons in repulsively interacting TBEC in [23]Na and [87]Rb [20]. Dark solitons in TBEC for a miscible case have also been analyzed recently [21]. TBEC in two different atoms has been produced in a system of [41]K and [87]Rb, in which sympathetic cooling of the Rb atoms was used to condense the K atoms [22]; as also in [7]Li-[133]Cs [23]. Keeping in mind the

importance of the matter wave solitons for Bose-Einstein condensates |2] , we present exact solutions of the generic TBEC model, for the low density limit. However, for the strong coupling limit, we solved the coupled GP equations numerically for both attractive and repulsive cases.

Derivation of the TBEC coupled GP equations: To derive the coupled GP equations of TBEC we assume that both the components of are confined in a cylindrical harmonic potential $V = m\omega_\perp(x^2 + y^2)/2$. By assuming that there is no confinement along z axis, we can reduce the problem to a quasi-1D one. Thus the double component wavefunction can be written as $\Psi_a = f_a(z,t)g(x,y,\sigma(z,t))$, $\Psi_b = f_b(z,t)g(x,y,\sigma(z,t))$, such that

$$\sigma(z) = \int dxdy[|\Psi_a|^2 + |\Psi_b|^2] = |f_a|^2 + |f_b|^2. \tag{4.12}$$

In Eq. (4.12), we have used the normalization condition on g. The action for the TBEC can be written as:

$$S = \int [i\hbar\Psi_a^\dagger \frac{\partial\Psi_a}{\partial t} + i\hbar\Psi_b^\dagger \frac{\partial\Psi_b}{\partial t} - \frac{\hbar^2}{2m}(\nabla\Psi_a^\dagger).(\nabla\Psi_a) - \frac{U_0}{2}(|\Psi_a|^2 + |\Psi_b|^2)^2 -$$
$$\frac{\hbar^2}{2m}(\nabla\Psi_a^\dagger).(\nabla\Psi_a) - V(x,y)(|\Psi_a|^2 + |\Psi_b|^2)]drdt. \tag{4.13}$$

Minimizing Eq. (4.13) w.r.t g^*, we find that

$$-\frac{\hbar^2}{2m}\nabla^2 g + Vg + U_0\left[(|f_a|^2 + |f_b|^2)|g|^2\right]g +$$
$$\frac{\hbar^2}{2m(|f_a|^2 + |f_b|^2)}\left[|\frac{\partial f_a}{\partial z}|^2 + |\frac{\partial f_b}{\partial z}|^2\right]g = \mu(\sigma)g \tag{4.14}$$

where μ is the chemical potential. We neglect the last term in Eq. (4.14) since the characteristic length of the pulses is sufficiently long that it is negligible in all cases of interest. For the same reason the term $f_a\nabla g$ is **equal to**

$$f_a\nabla_\perp g + \hat{z}f_a\frac{\partial g}{\partial z} \sim f_a\nabla_\perp g, \tag{4.15}$$

where

$$\nabla_\perp = \hat{x}\frac{\partial}{\partial x} + \hat{y}\frac{\partial}{\partial y}, \tag{4.16}$$

with x, y and z being the unit vectors in the directions x, y and z respectively. Thus, Eq. (4.14) reduces to

$$-\frac{\hbar^2}{2m}\nabla_\perp^2 g + Vg + U_0[(|f_a|^2 + |f_b|^2)|g|^2 g = \mu(\sigma)g \qquad (4.17)$$

Now minimizing Eq. (4.13) w.r.t f_a^* we find that

$$i\hbar\frac{\partial f_a}{\partial t} = -\frac{\hbar^2}{2m}\frac{\partial^2 f_a}{\partial z^2} + \left(\frac{\hbar^2}{2m}\int |\nabla_\perp g|^2 \, dxdy\right) f_a$$
$$+ U_0\left(\int |g|^4 \, dxdy\right)(|f_a|^2 + |f_b|^2)f + \left(\int |g|^2 V dxdy\right) f_a. \qquad (4.18)$$

Similarly, one can obtain the equation for f_b.

For the homogeneous medium assuming $f_a = \sigma_a^{1/2}\exp(i\phi_a)$, and $//, = \sigma_b^{1/2}\exp(i\phi_b)$ and defining the velocity field associated with f_a, and f_b as $v_a - \hbar/m\partial_z\phi_a$, and $v_b = \hbar/m\partial_z\phi_b$ we obtain the following equation for μ:

$$\mu(\sigma) = \left(\frac{\hbar^2}{2m}\int |\nabla_\perp g|^2 \, dxdy\right) + \left(\int |g|^2 V dxdy\right)$$
$$+ U_0\left(\int |g|^4 \, dxdy\right)(|f_a|^2 + |f_b|^2). \qquad (4.19)$$

Weak coupling limit:

To derive the coupled GP equations in the low density limit, we assume that the nonlinearity is weak , and hence only concentrate on the linear part of the Schrodinger equation satisfied by g, in a harmonic trap

$$-\frac{\hbar^2}{2m}\nabla_\perp^2 g + Vg = \mu g$$

This implies

$$|g| \propto \exp\left(-\frac{x^2 + y^2}{2a_\perp^2}\right).$$

From Eq. (4.19) we find that

$$\mu = \left(\frac{\hbar^2}{2m}\int |\nabla_\perp g|^2 \, dxdy\right) + \left(\int |g|^2 V dxdy\right);$$
$$|g|^2 = \exp\left(-\frac{x^2 + y^2}{2a_\perp^2}\right).$$

We also note that $a\pm = (\hbar/m\omega_\perp)^{1/2}$. After performing **the** integrals, we obtain

$$\mu = (1 + 2a\sigma)\hbar\omega;$$

where the first term corresponds to ground state energy and the second term correspond to the interaction energy. Thus the equation for f_a can be **written** as

$$i\hbar\partial_t f_a = -\frac{\hbar^2}{2m}\partial^2{}_x f_a + \hbar\omega_\perp \left[1 + 2a_{\mathrm{sc}}(|f_a|^2 + |f_b|^2)\right] f_a.$$

By performing these transformations

$$f_a = w_a e^{i\omega_\perp(1 + 2a\sigma_0)t},$$

and

$$f_b = w_b e^{-i\omega_\perp(1 + 2a\sigma_0')t},$$

we obtain the GP equations for one species of the TBEC, in the low density limit as

$$i\hbar\partial_t w_a = -\frac{\hbar^2}{2m}\partial_x^2 w_a + \varepsilon[|w_a^2| + |w_b^2|]w_a - \epsilon_a w_a. \tag{4.20}$$

By implementing the same procedure we can obtain the GP equation for the second component also as

$$i\hbar\partial_t w_b = -\frac{\hbar^2}{2m}\partial_x^2 w_b + \varepsilon[|w_a^2| + |w_b^2|]w_b - \epsilon_b w_b. \tag{4.21}$$

Here, $\varepsilon = 2\hbar\omega_\perp a$, ϵ_a and ϵ_b are the chemical potentials of the two species respectively. This scenario is similar to the much studied Manakov system [1, 24], which is integrable system. By writing $w_a = \sqrt{\sigma_a}e^{i(\phi_a + w_a t)}$, and $w_b = \sqrt{\sigma_b}e^{i(\phi_b + w_b t)}$; we can separate the real and imaginary parts of Eqs. **(4.20)** and (4.2$!), and obtain the two equations

$$v_a = u + \frac{c_1}{\sigma_a},$$

and

$$v_b = u + \frac{c_2}{\sigma_b}$$

where c_1, and c_2 are the integration constants. We assumed that both σ, and *(p* are functions of *(z - ut)*. Use was also made of the superfluid velocity $v_a = \frac{\hbar}{m}\partial_z\phi_a$ similarly, for v_b. Plugging the above results into the real parts one obtains

$$\frac{d^2\sigma_a}{dz^2} = \frac{1}{2\sigma_a}(\frac{d\sigma_a}{dz})^2 + \frac{4M\varepsilon}{\hbar^2}(\sigma_a + \sigma_b)\sigma_a - \frac{4M}{\hbar^2}\epsilon_a\sigma_a - \frac{2M^2u^2}{\hbar^2}\sigma_a + \frac{2M^2c_1^2}{\hbar^2\sigma_a} - \frac{4M\omega_a}{\hbar}\sigma_a, \tag{4-22}$$

$$\frac{d^2\sigma_b}{dz^2} = \frac{1}{2\sigma_b}(\frac{d\sigma_b}{dz})^2 + \frac{4M\varepsilon}{\hbar^2}(\sigma_a+\sigma_b)\sigma_b - \frac{4M}{\hbar^2}\epsilon_b\sigma_b - \frac{2M^2u^2}{\hbar^2}\sigma_b + \frac{2M^2c_2^2}{\hbar^2\sigma_b} - \frac{4M\omega_b}{\hbar}\sigma_b. \tag{4-23}$$

One finds both chirped and non-chirped $(c_i \neq 0)$ solutions of the above coupled equations. These are in the form of elliptic functions. The repulsive and attractive cases show distinct behavior for certain values of the modulus parameter *fn.*

4.5 Exact solutions

In this section we present the exact periodic solutions of the coupled equations (4.22) and (4.23) in terms of Jacobi elliptic functions with appropriate modulus parameter. It is well-known that these elliptic functions interpolate between the trigonometric and the hyperbolic functions for *fn* = 0, and $m = 1$ respectively. We start with a more general solution of Eqs. (4.22) and (4.23), which, for various limiting conditions of the parameter values, yields traveling solutions:

$$\sigma_a = A + B\gamma^2\mathrm{cn}^2(\alpha\gamma(z- ut),\tilde{m}),$$

$$\sigma_b - C + D\gamma^2\mathrm{sn}^2(\alpha\gamma(z - ut),fn).$$

Then it is clear that the coefficients of $\mathrm{cn}^n(z - ut,\tilde{m})$, and $\mathrm{sn}^n(z - ut,\tilde{m})$ for $n = 0, 2, 4, 6$ respectively, can be set to zero to reduce the problem to a set of eight algebraic equations, and obtain the solution. The identities satisfied by these cnoidal functions are handy in finding the solutions.

The consistency conditions for both σ_a, and σ_b are:

$$2AB\alpha^2\gamma^4(1-m) + A^2\alpha_2 + \frac{2M^2u^2}{\hbar^2}A^2 + \frac{4M\omega_a}{\hbar}A^2 - $$
$$\Gamma A^2C - \Gamma A^3 - \Gamma AD\gamma^2 - \delta = 0,$$

$$4B\alpha^2\gamma^2(2m-1) + \Gamma AD + 2\alpha_2 B + \frac{4M^2u^2}{\hbar^2}B + $$
$$\frac{8M\omega_a}{\hbar}B - 2\Gamma BC - 2\Gamma BD\gamma^2 - 3\Gamma AB = 0,$$

$$6A\alpha^2m - 2B\alpha^2\gamma^2(2m-1) - 2\Gamma AD - $$
$$\frac{2M^2u^2}{\hbar^2}B - B\alpha_2 - \frac{4M\omega_a}{\hbar}B + \Gamma BC + \Gamma BD\gamma^2 + 3\Gamma AB = 0,$$

$$4\alpha^2m - \Gamma D + \Gamma B = 0.$$

$$2CD\alpha^2\gamma^4 + C^2\alpha_2 + \frac{2M^2u^2}{\hbar^2}C^2 + \frac{4M\omega_b}{\hbar}C^2 - $$
$$\Gamma C^2A - \Gamma C^3 - \Gamma BC^2\gamma^2 - \delta_1 = 0,$$

$$-4D\alpha^2\gamma^2(m+1) + \Gamma BC + 2\alpha_2 D + \frac{4M^2u^2}{\hbar^2}D + $$
$$\frac{8M\omega_a}{\hbar}D - 2\Gamma AD - 2\Gamma BD\gamma^2 - 3\Gamma CD = 0,$$

$$6C\alpha^2m - 2D\alpha^2\gamma^2(m+1) + 2\Gamma BC + $$
$$\frac{2M^2u^2}{\hbar^2}D + D\alpha_1 + \frac{4M\omega_b}{\hbar}D - \Gamma AD - \Gamma BD\gamma^2 - 3\Gamma DC = 0,$$

$$4\alpha^2m - \Gamma D + \Gamma B = 0.$$

Here, $\Gamma = \frac{4M\epsilon}{\hbar^2}$, $\alpha_2 = \frac{4M\epsilon_a}{\hbar^2}$, $\alpha_1 = \frac{4M\epsilon_b}{\hbar^2}$, $\delta = \frac{2M^2c_1^2}{\hbar^2}$, and $\delta_1 = \frac{2M^2c_2^2}{\hbar^2}$.

Without chirping.

Case(i): Hyperbolic solutions. -

For $A = 0$, and $C = 0$ imply $c_1 = 0$, and $c_2 = 0$. For $\bar{m} - 1$ one obtains

$$\sigma_a = B\gamma^2\text{sech}^2(\alpha\gamma(z - ut)),$$

$$\sigma_b = D\gamma^2\text{tanh}^2(\alpha\gamma(z - ut)),$$

where

$$D = \frac{2\alpha^2\gamma^2 + \frac{4M\epsilon_a}{\hbar^2} + \frac{4M\omega_a}{\hbar}}{\Gamma\gamma^2},$$

and

$$B = \frac{-4\alpha^2\gamma^2 + \frac{4M\epsilon_b}{\hbar^2} + \frac{4M\omega_b}{\hbar}}{\Gamma\gamma^2}.$$

The width of the solitons is constrained by the condition

$$\alpha\gamma = \sqrt{\frac{2M}{\hbar^2}(\epsilon_a - \epsilon_b) + \frac{2M}{\hbar}(\omega_a - \omega_b)}.$$

Case(ii): Trigonometric solution. -

For $m = 0$, it is observed that both the fields have same amplitudes. Furthermore, the solutions are constrained by the condition $\epsilon_a + \hbar\omega_a = \epsilon_b + \hbar\omega_b$.

$$\sigma_a = B\gamma^2\cos^2(\alpha\gamma(z - ut)),$$

$$\sigma_b = D\gamma^2\sin^2(\alpha\gamma(z - ut)),$$

where

$$B = D = \frac{-2\alpha^2\gamma^2 + \frac{4M\epsilon_b}{\hbar^2} + \frac{4M\omega_b}{\hbar}}{\Gamma\gamma^2}.$$

Case(iii): Pure cnoidal function. -

For any value of m, one obtains the pure cnoidal solutions as

$$\sigma_a = B\gamma^2\text{cn}^2(\alpha\gamma(z - ut), \tilde{m}),$$

$$\sigma_b = D\gamma^2\text{sn}^2(\alpha\gamma(z - ut), \tilde{m}),$$

where

$$B = \frac{-2\alpha^2\gamma^2(1 + m) + \frac{4M\epsilon_b}{\hbar^2} + \frac{2M^2u^2}{\hbar^2}\frac{4M\omega_b}{\hbar}}{\Gamma\gamma^2},$$

$$D = \frac{2\alpha^2\gamma^2(2m - 1) + \frac{4M\epsilon_a}{\hbar^2} + \frac{2M^2u^2}{\hbar^2}\frac{4M\omega_a}{\hbar}}{\Gamma\gamma^2}.$$

In the static case $(u = 0)$, under the limits $(\tilde{m} = 0, 1)$, the respective amplitudes of the solitary waves get modified leaving the relationship of the chemical potentials with the frequencies and the widths unaffected.
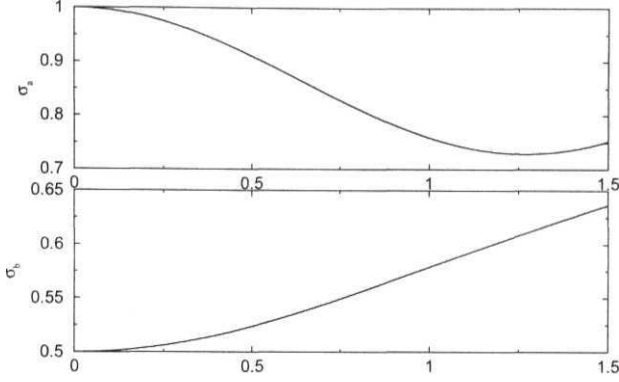
Figure **4.2:** **Plot** depicting the amplitudes of TBEC (weak coupling) for $E = 0.4$, $\epsilon_a = 0.8$, $\epsilon_b = 0.02$, $\sigma_a^0 = 1.0$, $\sigma_b^0 = 0.5$, and $u = 0.8$

Chirping pulses.-

Case(i): **Hyperbolic** case.-

We assume **that, there** is no chirping of the σ_b field, hence, $C = 0$. This case yields a hyperbolic solution with chirping in σ_a field for $D - 1$.

$$\sigma_a = A + B\gamma^2 \text{sech}^2(\alpha\gamma(z - ut)),$$

$$\sigma_b = \gamma^2 \tanh^2(\alpha\gamma(z - ut)),$$

where, $A = (1 - \frac{4\alpha^2}{\Gamma})[\Gamma\gamma^2(1 - \frac{4\alpha^2}{\Gamma}) - P]/Q$, with $P = -2\alpha^2\gamma^2 + \frac{4M\epsilon_a}{\hbar^2} + \frac{4M\omega_a}{\hbar} + \frac{2M^2 u^2}{\hbar^2}$, $Q = 6\alpha^2 - \Gamma$, and $B = 1 - \frac{4\alpha^2}{\Gamma}$.

Figure 4.3: Plot depicting the amplitudes of TBEC (weak coupling) for E -1.0, $\epsilon_a = 0.8$, $\epsilon_b = 0.02$, $\sigma_a^0 = 1.0$, $\sigma_b^0 = 0.5$, and $u = 0.8$
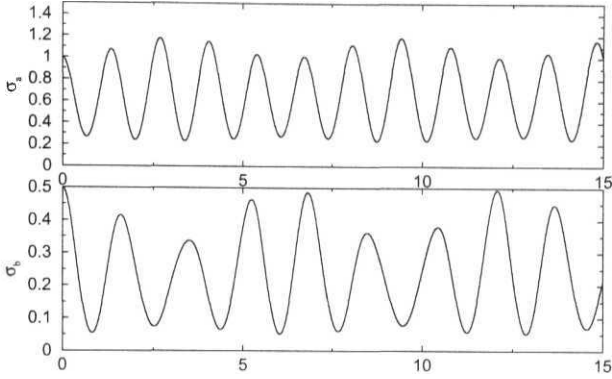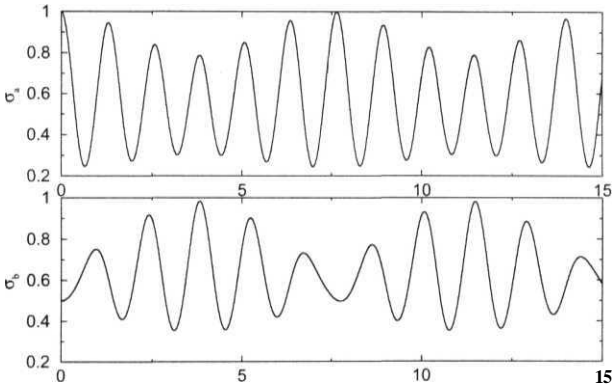

Figure 4.4: Plot depicting the amplitudes of TBEC (weak coupling) for $E =$ -1.0, $\epsilon_a = 0.8$, $\epsilon_b = 0.02$, $\sigma_a^0 = 1.0$, $rf = 1.0$, and $u = 0.8$

Strong coupling limit:

We take the TF limit. For large nonlinearities U_0, and thus for high particle density, and high self energy in real experiments for BEC, the kinetic term becomes small. Hence it can be neglected. We then get a simple analytic solution for $\Psi(r,t)$. It is observed that for the harmonic trap, the population density goes to zero at $r = \pm 2/\alpha\sqrt{\mu}$, where $\alpha^2 = 2m\omega_\perp$. Consequently, the normalization condition is

$$\int |g|^2 \, dx dy = 1.$$

In certain cases, for the eigenstates of a harmonic trap, the wavefunction can be written as

$$\Psi_a(r,t) = \Psi_a(r)e^{-i\mu t/\hbar}$$

with eigenvalue μ representing the chemical potential at zero temperature. Substituting this into the GP equation, we get

$$\mu\Psi_a = [-\frac{\hbar^2}{2m}\nabla^2 + V + U_0(|\Psi_a^2| + |\Psi_b^2|)]\Psi,$$

Thus, for harmonic trap, in the TF approximation we get

$$\mu = \alpha^2\frac{r^2}{4} + U_0[|f_a|^2 + |f_b|^2]|g|^2.$$

The normalization condition implies that

$$2\pi\int_0^{2/\alpha\sqrt{\mu}} dr\frac{r}{\sigma U_0}[\mu - \alpha^2\frac{r^2}{4}] = 1.$$

This integral is solved to give

$$\mu = 2\hbar\omega_\perp(\sigma a)^{1/2}.$$

Substituting this into Eq. (4.18) yields

$$i\hbar\partial_t f_a = -\frac{\hbar}{2m}\partial^2_x f_a + 2\hbar\omega_\perp a^{1/2}[|f_a|^2 + |f_b|^2]^{1/2}f.$$

By applying another transformation $f_a = w_a e^{2i\omega_\perp \sigma_0 t}$, and $f_b = w_b e^{2i\omega_\perp \sigma_0' t}$ we obtain the GP equation for strong coupling case

$$i\hbar \partial_t w_a = -\frac{\hbar^2}{2m}\partial_x^2 w_a + \varepsilon[|w_a|^2 + |w_b|^2]^{1/2}w_a - \epsilon_a w_a.$$

By extending the same procedure , we also derive the GP equation for w_b:

$$i\hbar \partial_t w_b = -\frac{\hbar^2}{2m}\partial_x^2 w_b + \varepsilon[|w_a|^2 + |w_b|^2]^{1/2}w_b - \epsilon_b w_b.$$

We again write $w_a = \sqrt{\sigma_a}e^{i(\varphi + w_a)}$, and $w_b = \sqrt{\sigma_b}e^{i(\varphi + w_b)}$ we can separate the real and imaginary parts. The real parts of the two coupled equations are given by

$$\frac{d^2\sigma_a}{dz^2} = \frac{1}{2\sigma_a}\left(\frac{d\sigma_a}{dz}\right)^2 - \frac{4m^2 u^2}{\hbar^2}\frac{(\sigma_a - \sigma_a^0)}{\sigma_a}\sigma_a^0 + \frac{4m\varepsilon}{\hbar^2}(\sigma_a + \sigma_b)^{1/2}\sigma_a - \frac{4m}{\hbar^2}\epsilon_a \sigma_a$$

$$\frac{d^2\sigma_b}{dz^2} = \frac{1}{2\sigma_b}\left(\frac{d\sigma_b}{dz}\right)^2 - \frac{4m^2 u^2}{\hbar^2}\frac{(\sigma_b - \sigma_b^0)}{\sigma_b}\sigma_b^0 + \frac{4m\varepsilon}{\hbar^2}(\sigma_a + \sigma_b)^{1/2}\sigma_b - \frac{4m}{\hbar^2}\epsilon_b \sigma_b.$$

4.6   Numerical results

The numerical evolution of these solutions reveal different behavior for attractive $(e < 0)$ and repulsive cases. In Fig. 4.2 the amplitudes for the repulsive case are plotted. On the other hand the attractive case is very interesting. As depicted in Fig.4.3 and Fig. 4.4 for suitable values of the parameters, one finds oscillatory solutions and a chirped oscillatory solutions. It should be noted that for the aforementioned cases, the integration constants are nonzero.

In the high density limit, the attractive case is very interesting. As depicted in Fig.4.5, for appropriate values of the parameters, one finds that σ_a is an oscillatory solution whereas σ_b shows *auto-correlation* traces of pulse trains generated by the induced modulational instability [25]. It is indeed, illuminating to note that these autocorrelation traces are observed when the pumping Nd:YAG laser and side-band InGaAsP semiconductor are coupled to single-mode fiber having zero-dispersion wavelength
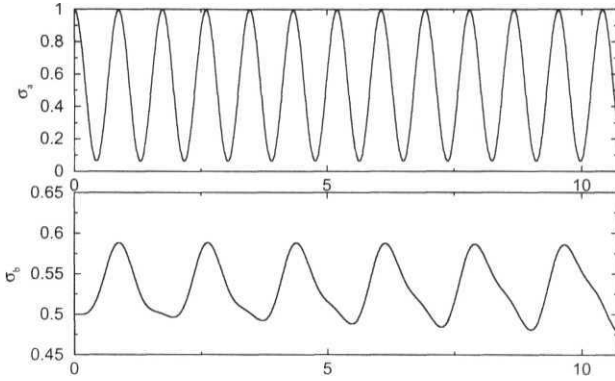
Figure 4.5: The upper panel depicts the oscillatory pulse trains, and the lower panel depicts the autocorrelation traces of pulse trains of TBEC generated by the induced modulational instability; for $e = -1.0$, $\epsilon_a = 5.0$, $\epsilon_b = 0.02$, $\sigma_a^0 = 1.0$, $\sigma_b^0 = 1.0$, and $u = 0.8$
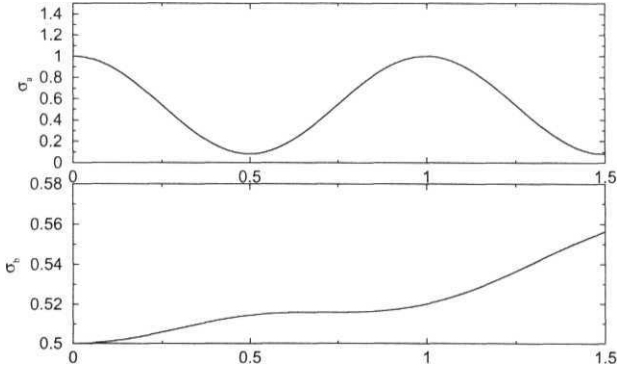

Figure 4.6: Plot depicting the amplitudes of TBEC for $E = 0.4$, $\epsilon_a = 5.0$, $\epsilon_b = 0.02$, $\sigma_a^0 = 1.0$, $\sigma_b^0 = 0.4$, and $u = 0.9$.

at $\lambda_0 - 1.275\mu m$. Furthermore, for repulsive interaction in a suitable range of parameter values, σ_a, σ_b are still oscillatory and the same has been depicted in Fig. 4.6.

References

[1] S.V. Manakov, Sov. Phys. JETP 38, 248 (1974).

[2] F. Dalfovo, S. Giorgini, L.P. Pitaevskii, and S. Stringari, Rev. Mod. Phys. **71,** 463 (1999).

[3] W.P. Reinhardt and C.W. Clark, J. Phys. **B217,** L785 (1997).

[4] W.P. Reinhardt, *Tunneling in Complex Systems*, S. Tomsovic, Ed. (World Scientific, Singapore, 1998).

[5] R. Dum, J. I. Cirac, M. Lewenstein, and P. Zoller, Phys. Rev. Lett. 80, 2972 (1998).

[6] V.M. Perez-Garcia, H. Michinel, and H. Herrero, Phys. Rev. A 57, 3837 (1998).

[7] O. Zobay, S. Potting, P. Meystre, and E.M. Wright, Phys. Rev. A 59, 643 (1999).

[8] P.O. Fedichev, A.E. Murshyev, and G.V. Shlyapnikov, Phys. Rev. A 60, 3220 (1999).

[9] A.E. Murshyev, H.B. van Linden van den Heuvell, and G.V. Shlyapnikov, Phys. Rev. A 60, R2665 (1999).

[10] T. Busch and J. Anglin, cond-mat/9809408.

[11] S. Burger, K. Bongs, S. Dettmer, W. Ertmer, and K. Sengstock, Phys. Rev. Lett. 83, 5198 (1999).

[12] W. D Philips and K. Helmerson (Unpublished).

[13] K.E. Strecker, G.B. Partridge, and A.G. Truscott, Nature (London) **417,** 150 (2002).

[14] G.M. Kavoulakis and C.J. Pethick, Phys. Rev. A 58, 1563 (1998).

[15] A.D. Jackson, G.M. Kavoulakis, and C.J. Pethick, Phys. Rev. A 58, 2417 (1998).

[16] A.D. Jackson and G.M. Kavoulakis, Phys. Rev. Lett. 89, 070403 (2002).

[17] T.-L. Ho and V.B. Shenoy, Phys. Rev. Lett. **77,** 3276 (1996).

[18] H. Pu and N.P. Bigelow, Phys. Rev. Lett. 80, 1130 (1998).

[19] D.S. Hall, M.R. Matthews, J.R. Ensher, C.E. Wieman, and E.A. Cornell, Phys. Rev. Lett. 81, 1539 (1998).

[20] Th. Busch and J.R. Anglin, Phys. Rev. Lett. 87, 010401 (2001).

[21] P. Ohberg and L. Santos, Phys. Rev. Lett. 86, 2918 (2001).

[22] G. Modugno *et al.* Science **294,** 1320 (2001).

[23] M. Mudrich *et al.* Phys. Rev. Lett. 88, 253001 (2002).

[24] R. Radhakrishnan, M. Lakshamanan, and J. Hietarinta, Phys. Rev. E **56**, 2213 (1997).

[25] A. Hasegawa, *Optical Solitons in Fibers* (Springer-Verlag, New York, 1990).

Chapter 5

Models for disoriented chiral condensates

5.1 Equilibrium and non-equilibrium pictures

Formation of domains below critical temperature is common to physical systems exhibiting second order phase transition. The order parameter having zero average in the symmetric high temperature phase, develops a vacuum expectation value below the critical temperature. It is worth mentioning that the effective field theories governing the second order phase transition are nonlinear in nature, an explicit example of the same and its implications will be seen below. There is a possibility of having domains with the order parameter orienting along different directions, in the broken symmetry phase. The domains in a ferromagnet, below the Curie temperature, are the prime examples of this scenario.

The chiral phase transition in quantum chromodynamics (QCD), provides an opportunity for the realization of the above type of domain formation. This phase transition, originating from the spontaneous breaking of the chiral symmetry, leads to the existence of pseudo scalar mesons e.g., pions. The chiral order parameter in a given domain is disoriented from the zero temperature vacuum direction σ; therefore these type of space-time

domains are called disoriented chiral condenstes (DCC). The eventual decay of these metastable DCC would lead to the production of pions, whose number distributions may be quite different from the expected proportion of 1/3 for each of the pion species in non-coherent production. A key motivation behind the search of DCC has been the Centauro events [1], where the neutral pion fraction /, has been observed to be more than the expected value 1/3. There also have been reports of anti-Centauro events [2]. An opportunity for the experimental realization of DCC is provided by the collison of heavy ions at high energy, where there is a possibility of restoring the spontaneously broken chiral symmetry.

In the absence of baryons, the pion dynamics is captured by the 0(4) σ-model with the Lagrangian,

$$L = \frac{1}{2}[(\partial_\mu \sigma)^2 + (\partial_\mu \pi_a)^2] - \frac{\lambda}{4}[\sigma^2 + \pi_a^2 - v^2]^2 + H\sigma. \tag{5.1}$$

The last term breaks the *0(4)* symmtery explicitly and is responsible for the masses of the pions. This model provides the starting point for various scenarios of DCC formation [3], which can be broadly classified into equilibrium and non-equilibrium pictures.

In the baked Alaska model of DCC, proposed initially by Bjorken [4], the high multiplicity ultra-high energy hadronic collisions lead to a rapidly expanding hot partonic shell. In its interior the chiral field may get misaligned from the true vacuum resulting in the formation of DCC. As pointed out earlier, depending on the direction of the order parameter in the domain, the resulting distribution of coherent pions, originating from the decay of the domain, can be substantially different from those of the incoherent pions originating from a regular plasma.

This is the most discussed signature of DCC. Defining the ratio of neutral pions to all pions by

$$f = \frac{n_{\pi_0}}{n_{\pi_0} + n_{\pi_\pm}}, \tag{5.2}$$

it has been shown that, the probability distribution for / can take a form

$$P(f) = \frac{1}{2\sqrt{f}}. \tag{5.3}$$

This distribution arises from the assumption that all points on the manifold S^3, representing σ, π_1, π_2 and π_3 fields, are equally likely as initial conditions. The number of pions of a given Cartesian isospin is taken to be proportional to *n'f, i* being the component of the isospin. It should be pointed out that the above distribution is appropriate only when all the pions are produced from a single domain. If pions are incoherently produced then the probability distribution /, will be a Gaussian peaked around the value 1/3. The above distribution differs markedly from the Gaussian one, especially for lower values of /. Probability for very small value of / is negligible for incoherent emission of pions, while it can be substantial for the DCC case. Hence, significant departure from the value 1/3 for / is the cleanest signal for the formation of DCC.

The fact that pions have finite mass leads to a small correlation length and hence small domains, of the order of m_π^{-1}, in the equilibrium picture of DCC formation. This has led to the nonequilibrium, quenching picture of DCC formation by Rajagopal-Wilczek [5] in the relativistic heavy ion collisions. In this scenario, the expansion of highly relativistic debris from the heavy ion collisions lead to the quenching of high temperature field configurations and therefore to the growth of long wavelength modes in time. These then give rise to large correlated DCC domains, leading to coherent low energy pions. Here the DCC domains after getting detached from the heat bath evolve according to the zero temperature equations of motion [3, 5, 6]. Here dramatic signals like the above mentioned fluctuations in the ratio of the neutral pions to all pions may not arise. An annealing scenario for DCC formation has also been proposed [7]. The role of fluctuations above T_G (Ginzburg temperature), in destabilizing the DCC in the conventional picture has also been analyzed [8].

A first order transition which may be a possibility in the chiral phase transition, can also give rise to DCC domains [9]. Recently in Ref. [10], the authors have demonstrated that a first order transition naturally leads to a quench like scenario, which is conducive to the growth of DCC domains.

The ability to detect DCC depends on their lifetime. The perfect non-equilibrium quenching scenario of Rajagopal and Wilczek, leads to the dissipation of the condensate. This is due to the possible energy exchange between different degrees of freedom, after the chiral condensate detaches from the heat bath, and evolves according to the zero temperature equations of motion. This problem has been recently studied [11, 12, 13, 14] for ascertaining various type of signals of DCC. Interestingly, a recent experiment, involving heavy-ions has hinted at the possibility of DCC formation [15, 16].

In the non-equilibrium picture of DCC formation in heavy ion collisions, one looks for extended solutions of the classical equations of motion, originating from the σ-model Lagrangian given above. In the linear σ-model, the potential responsible for the spontaneous breaking of chiral symmetry, introduces nonlinearity in the equations of motion. Because of the *nonlinearity,* it is difficult to obtain analytical solutions for the time evolution of the field configurations in $(3 + 1)$-dimensions. Hence, one starts with the idealized Heisenberg-type boundary conditions [17].

The thin disc representing Lorentz-contracted nuclei at the time of collision is assumed to be infinite in extent in the transverse directions. Assuming the fields to be independent of the transverse directions, one can simplify the problem to a $(1 + 1)$-dimensional field theory [6]. To obtain boost invariant solutions, which can lead to DCC formation, we resort to numerical methods. It should be pointed out that the existence of a central-plateau structure in the rapidity distribution of particles produced in cosmic ray events [18] and pp or pp collisions [19] has led to the assumption of an approximate $(1 + 1)$- Lorentz invariance.

5.2   Boost invariant solutions

Recently, Z. Wang *et al.* [20, 21] have studied the cluster structure of DCC, in the nonequilibrium picture, by solving the equations of motion corresponding to linear sigma model numerically. We will follow their approach in our simulations. After reproducing their results, we will investigate the scenario in which quenching takes the field to low enough a temperature, where the magnitude of the order parameter is constant, leaving the phase as the dynamical variable. In order to validate the initial conditions more appropriate to relativistic heavy ion collisions, they have neglected the transverse dimensions, and have assumed that Φ is only a fuction of t, and z.

In order to look for boost invariant solutions, the proper time $r = \sqrt{t^2 - z^2}$, and rapidity $\eta = \frac{1}{2}ln\frac{t+z}{t-z}$, variables are introduced. We note that

$$[\frac{\partial^2}{\partial t^2} - \frac{\partial^2}{\partial z^2}] \rightarrow [\frac{1}{\tau}\frac{\partial}{\partial \tau}(\tau\frac{\partial}{\partial \tau}) - \frac{1}{\tau^2}\frac{\partial^2}{\partial \eta^2}]. \tag{5.4}$$

The equations of motion read

$$[\frac{1}{\tau}\frac{\partial}{\partial \tau}(\tau\frac{\partial}{\partial \tau}) - \frac{1}{\tau^2}\frac{\partial^2}{\partial \eta^2}]\sigma = -\lambda\sigma(\sigma^2 + \pi^2 - v^2) + H \tag{5.5}$$

$$[\frac{1}{\tau}\frac{\partial}{\partial \tau}(\tau\frac{\partial}{\partial \tau}) - \frac{1}{\tau^2}\frac{\partial^2}{\partial \eta^2}]\sigma = -\lambda\sigma(\sigma^2 + \pi^2 - v^2). \tag{5.6}$$

The simplest case to solve Eqs. (5.5) and (5.6) is when the system has Lorentz-boost invariance i.e.,

$$\phi(\tau_0, \eta) = \phi_0, \tag{5.7}$$

where ϕ_0 is independent of η. Since the starting point is the symmetric phase from where quenching is done, one takes the initial conditions as $\phi(\tau_0) = 0$. The other boundary condition taken by the above authors is $\partial\pi/\partial\tau = (1,5,0,0)$ MeV/fm, at $\tau_0 = 1$fm/c. The general feature of the solution is that the σ field grows from zero and takes about 1fm/c propertime
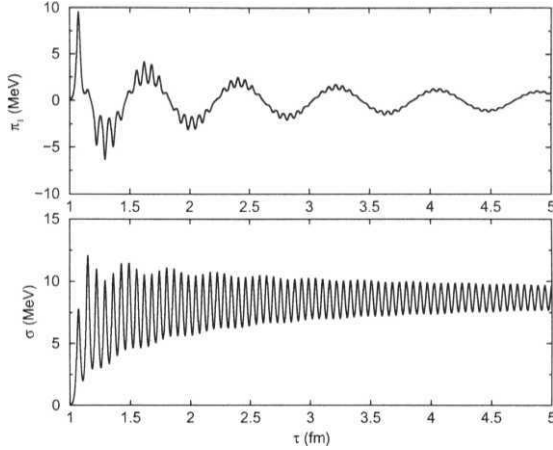
Figure 5.1: Proper time evolution of σ, and π_1 field following a Lorentz boost invariant initial condition at $\tau_0 = 1fm/c$, of the linear **sigma** model.

to reach the true vacuum expectation value $< \sigma >\sim f_\pi$. While the Φ field oscillates around zero rather slowly and eventually tends to zero when the proper time gets large.

5.3 DCC and sine-Gordon equation

It is of deep interest to enquire, as to what happens when the field configuration in the symmetric phase is quenched to a temperature, such that the magnitude of the order parameter has taken a contant value, leaving the phases as the dynamical variables. We assume that the field configuration evolves in the σ-π_3 plane, same as in the above scenario. In this case the explicit symmetry breaking term responsible for the pion mass affects the dynamics. The relevant eqation is the sine-Gordon equation given by

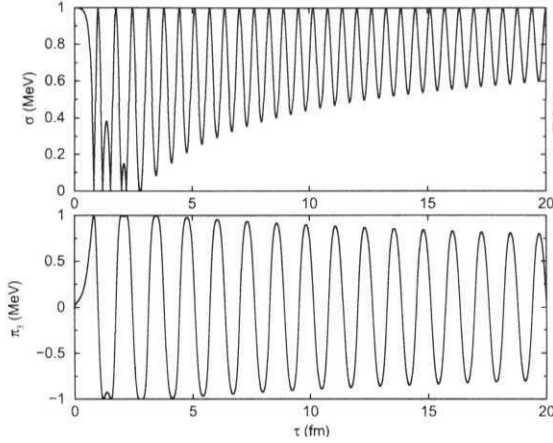$$\partial_\mu \partial^\mu \theta(x,t) + a\sin\theta(x,t) = 0, \tag{5.8}$$

Figure 5.2: Proper time evolution of σ, and π_3 field following a Lorentz boost invariant initial condition at $\tau_0 = 1 fm/c$, under SG equation.

where $a = \frac{\epsilon}{f_{\pi}2}$. The field variables are $\Phi = (a, \pi_3, 0, 0) = (\cos 0(z, t), \sin\theta(x, t), 0, 0)$. We have performed a numerical simulation with the boost invariant evolution of the initial field configuration as given in Ref. [20]. It was found, as indicated in Fig. (5.2), that, the σ field grows from zero and takes a longer propertime as compared to the previous case to reach the true vacuum expectation value $< \sigma > \sim f_{\pi}$. While the Φ field oscillates around zero rather slowly and eventually tends to zero when the proper time gets large.

Below we describe a soliton picture of DCC [22]. In this case, the solution does not preserve boost invariance. It is well-known that the $(1 + 1)$ sine-Gordon equation, possesses stable solitary wave solutions [23]. For example, the well-known kink and anti-kink solutions are: $\theta(\xi) = 4 \arctan[\exp \pm \gamma \xi]$. These domains can be potential candidates for DCC. It is interesting to point out that domains of Bose-Eintein condensates have been successfully modelled as the solitons and soliton trains of the relevant order parameter equation in $(1 + 1)$ dimensions. As long as the
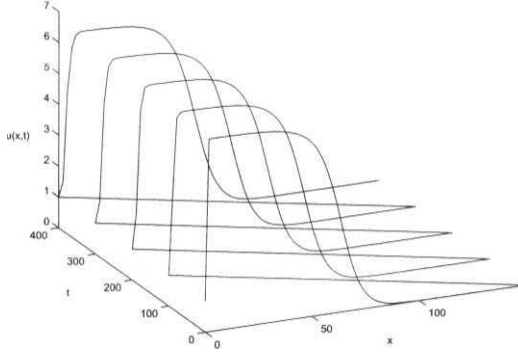
Figure 5.3: Classical evolution of domain in (1 + 1)-dimensions.

expansion is one dimensional the solitons are completely stable. Eventually, when the expansion becomes three dimensional, they decay into low-energy coherent pions, since no conservation law prevents it and these solutions have higher energy, as compared to the homogeneous vacuum solution. In the accompanying figure (Fig. 5.4), we depict the the results of the classical evolution of a coherent structure in (2 + 1)-dimensions. It clearly shows that, after sufficient time, the coherent structure breaks up into plane waves, representing pions. Below we give the numerical algorithm to solve the SG equation in $(2+1)$-dimension, by the symmetry it can be extended to the full space.

To solve the sine-Gordon equation in (2 + 1)-dimensions, we use the centered finite difference method to discretize the space and time variables. For this, we take $x = /\text{Ax}$; $y = j\triangle y$; $t = k\triangle t$ and the solution as

$$u_{i,j}^k = u(i\triangle x, j\triangle y, k\triangle t).$$

The adjoining figure corroborates our insights. Then the finite difference
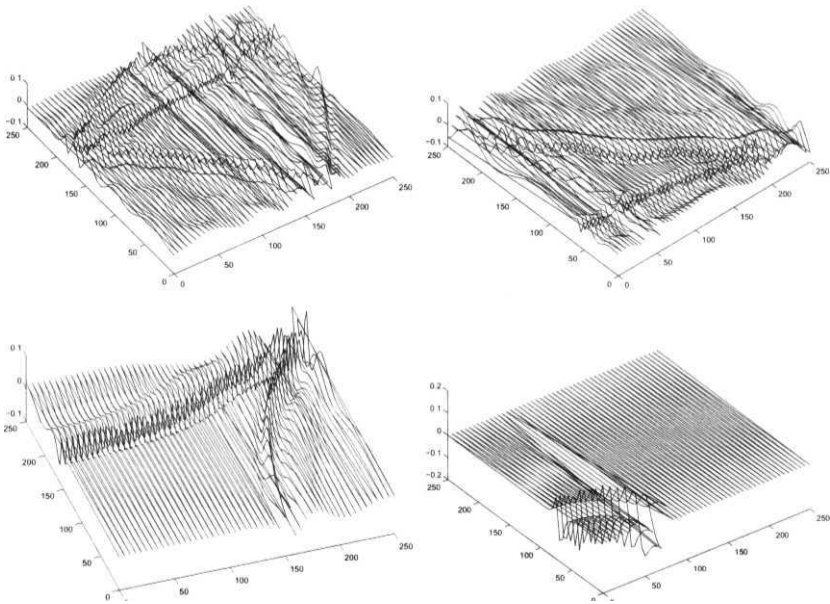
Figure 5.4: Classical evolution of a domain. The four frames correspond to times 100, 500, 800, and 1200 in appropriate units.

SGE takes the form

$$u_{i,j}^{k+1} = -u_{i,j}^{k-1} + 2[1 - 2(\frac{\triangle t}{\triangle x})^2]u_{i,j}^k + (\frac{\triangle t}{\triangle x})^2[u_{i+1,j}^k +$$

$$u_{i-1,j}^k + u_{i,j+1}^k + u_{i,j-1}^k] - (\triangle t)^2\sin[\frac{1}{4}(u_i^k + 1, j + u_{i-1,j}^k + u_{i,j+1}^k + u_{i,j-1)}^k)] \quad (5.9)$$

5.4   Traveling wave solutions of 0(4) sigma model

It is natural to ask about the possibility of solitary wave solutions in the O(4)-sigma model itself. These can be localized solitons, or periodic ones. It has been shown that [22], the σ-model Lagrangian, in the presence of an additional isospin violating terms quadratic in the field variables, *e.g.,* $\mu\pi_3^2$ (without the explicit symmetry breaking term) leads to stationary solutions of the type

$$\pi_1 = l\text{sech}\frac{\sqrt{2\mu}}{f_\pi}\xi,$$

$$\pi_2 = m\text{sech}\frac{\sqrt{2\mu}}{f_\pi}\xi,$$

$$\pi_3 = n\tanh\frac{\sqrt{2\mu}}{f_\pi}\xi,$$

$$and \quad \sigma = l\text{sech}\frac{\sqrt{2\mu}}{f_\pi}\xi, \quad (5.10)$$

where $\alpha^2 - 1 + \frac{\mu}{2\lambda}$, and $l^2 + m^2 + n^2 = 1 - \frac{\mu}{2\lambda}$. These type of inhomogeneous solutions can model DCC and the corresponding neutral pion fraction will differ significantly from the expected $1/\sqrt{7}$ distribution.

We now show that, in the absence of the additional quadratic term taken above, we can still find exact propagating wave solutions of the equations of motion for the $O(4)$ Lagrangian in $(1 + 1)$ dimensions. Like in the above case, we assume that the fields are decoupled from heat bath and pointing along σ, and π_3 directions. Then we find that the traveling wave solutions are given in terms of the cnoidal functions.

The equations of motion for the σ, and the π_3 fields in $(1+1)$-dimensions can be written as

$$\frac{d^2\sigma}{d\xi^2} + a\sigma^3 + a\sigma\pi_3^2 - a\sigma = 0, \tag{5.11}$$

$$\frac{d^2\pi_3}{d\xi^2} + a\pi_3^3 + a\sigma^2\pi_3 - a\pi_3 = 0. \tag{5.12}$$

where, $\xi = x - vt$, and $a = -\frac{4\lambda}{f_{\pi^2}(1-v^2)}$. Then we find that

$$\sigma = [1 + \frac{\alpha^2(1-2m)}{a}]^{1/2}\mathrm{sn}(\alpha\xi, m), \tag{5.13}$$

and

$$\pi_3 = [1 + \frac{\alpha^2}{a}]^{1/2}\mathrm{cn}(\alpha\xi, m), \tag{5.14}$$

where, m is the modulus parameter. These are periodic excitations of the order parameter. We hope that these type of excitations will be observed experimentally. It is interesting to note that in a single component BEC, these type of soliton trains have been seen experimentally.

References

[1] Chacaltaya-Pamir Collaboration; Tokyo University preprint ICRR-Report-258-91-27 and references therein.

[2] C.M.G. Lattes, Y. Fujimoto, and S. Hasegawa, Phys. Rep. 65, 151 (1980).

[3] A.A. Anselm, Phys. Lett. B **217,** 169 (1989); A.A Anselm and M.G. Ryskin, Phys. Lett. B **266,** 482 (1991).

[4] J.D. Bjorken, Int. J. Mod. Phys. A 7, 4189 (1987); Acta. Phys. Pol. B **23,** 561 (1992); K. Kowalski and C. Taylor, hep-ph/9211282.

[5] K. Rajagopal and F. Wilczek, Nucl. Phys. **B399,** 395 (1993); K. Rajagopal and F. Wilczek, Nucl. Phys. B **404,** 577 (1993).

[6] J.-P. Blaizot and A. Krzywicki, Phys. Rev. D **46,** 246 (1992).

[7] S. Gavin, A. Gocksch, and R.D. Pisarski, Phys. Rev. Lett. **72,** 2143 (1994).

[8] S. Digal and A.M. Srivastava, Mod. Phys. Lett. A **13,** 2369 (1998).

[9] J.I. Kapusta and A.P. Vischer, Z. Phys. C 75, 507 (1997).

[10] O. Scavenius and A. Dumitru, Phys. Rev. Lett. 83, 4697 (1999).

[11] A. Mocsy, Phys. Rev. D **66,** 056010 (2002).

[12] J. Serreau, hep-ph/0304011.

[13] S.M.H. Wang and J.I. Kapustaa, Nucl. Phys. A **715** 573 (2003).

[14] Y.Y. Charng, K.W. Ng, C.Y. Lin, and D.S. Lee, Phys. Lett. B **548,** 175 (2003).

[15] M.M. Aggarwal *etal,* Phys. Rev. C 64, 011901(R) (2001).

[16] J. Serreau, "Disoriented Chiral Condensate Formation in Heavy Ion Collisions?", Talk at TH-2002, "International conference on Theoretical Physics", UNESCO, Paris, France.

[17] W. Heisenberg, Z. Phys. **133,** 65 (1952).

[18] T.H. Burnett *et al.,*Phys. Rev. Lett. 50, 2062 (1983).

[19] F. Abe *et al.,*Phys. Rev. D **41,** 2330 (1990).

[20] Z. Wang, M. Suzuki, and X.N. Wang, Phys. Rev. D 50, 2277 (1994).

[21] Z. Haung and X.N. Wang Phys. Rev. D 49, 4335(R) (1994).

[22] P.K. Panigrahi and C. Nagaraja Kumar, *Solitons*, R. MacKenzie, M.B. Paranjape, and W.J. Zakrzewski (eds.) 163 (2000).

[23] R. Rajaraman, *Solitons and Instantons*, (North-Holland Publishing Co., Boston, 1982).

Chapter 6

Conclusions

In conclusion, this thesis dealt with the solutions of a wide class of non-linear equations, ranging from one relevant for the twin-core optical fibers to equations governing the dynamics of Bose-Einstein condensates and chiral phase transitions. The fact that, the underlying nonlinearity of these diverse systems are of similar nature, led to similar type of solutions in these otherwise unrelated physical systems. We gave a fractional transformation which connected the solutions of the phase-locked nonlinear Schrodinger equation with the elliptic functions. A recently developed method to incorporate dissipation and time dependence of the nonlinear coupling and varying dispersion has also been implemented for the NLSE phase locked with a source.

The existense of periodic solutions of a number of integrable systems like MKdV and NLSE naturally lead to the possibility of strictly finite compacton solutions in these type of systems. It should be noted that, KP and Boussinesq equations have been suitably modified in order that they support compacton solutions. It was found that the MKdV and NLSE equations need to be appended with suitable sources in order to possess compacton type solutions. It was numerically observed that these type of solutions are stable in NLSE with an appropriate source. Various other nonlinear equations where the above type of solutions are possible

were indicated. We have also presented rational periodic solutions of the Boussinesq equation using the same method of fractional transformation, as used for the above equations.

We have then examined the self-similar solutions of the two component Bose-Einstein condenstaes a subject of considerable theoretical and experimental interest in recent times. Chirped and unchirped solitary wave and localized soliton solutions were exhaustively analyzed in the quasi-one dimensional domain, starting from the relevant Gross-Pitaevskii equation. We have studied both weak and strong coupling regimes using analytic and numerical tools. In the weak coupling regime, the solutions involve the elliptic functions which interpolate between the trigonometric and hyperbolic functions as limiting cases. In the numerical front we have made use of semi-implicit Crank-Nicholson technique which is unconditionally stable. Apart from a number of intersting features we observe modulational instability characteristic of the ring laser in the two component BEC.

The subject of domain formation in the chiral phase transition of QCD was also investigated in the quench scenario. We studied the possibility of quenching leading to a situation, where the magnitude of the order parameter has stabilized, but the phase fluctuations are still present. In this case, the underlying dynamical equations, taking into consideration the pancake type geometry of the heavy ion collisions, leads to the well-known sine-Gordon equation in $1 + 1$ dimensions. Boost invariant solutions were studied numerically and were found to yield the same type of clusters. These clusters owe their origin to the phase fluctuations. We then elaborate on the possibility of the soliton solutions of the sine-Gordon equation describing disoriented chiral condensate. Keeping in mind the rather low temperature of the regime, where the magnitude of the order parameter has taken constant value, we evolve the soliton solutions of the sine-Gordon equation into the transverse directions. The coherent production of pions from the slow break up of the soliton in higher dimensions was

pointed out.

A number of directions can be pursued starting from the methods and results of this thesis. We have only investigated the solutions of NLSE phase-locked with a source. The general scenario, where phase of the source and the solution differ, is an area of active research, having applications in fiber optics and other areas. It has been seen numerically that, the well-known phenomenon called auto-resonance occurs in this system. It will be worthwhile to apply the procedure of fractional transformation developed here to these type and other nonlinear systems. Similarly, the effect of dissipation and space-time dependence of coupling and dispersion needs careful analysis. We have only dealt with elementary self-similar solutions for the two component BEC. Of late, the dynamics of soliton and soliton trains, is attracting considerable theoretical and experimental interest. The case of single component BEC has been investigated recently implying novel instability in this system. The same needs to be studied in the two component case. Since, it is well-known that the dynamics of this system is much more complex and correlated. The possibility of manipulation of phase of solitons, leading to the storage and retrieval of information in BEC, is an extremely promising area of research. Recently BECs have been treated as testing ground for checking ideas, ranging from, Hawking radiation, supernovae to quantum computation. We hope that some of the methods developed here may find application in the above endeavors.

Appendix

In this appendix, we briefly describe some properties of the three Jacobi elliptic functions and two of the complete elliptic integrals, having relevance to the works presented in this thesis.

$$\int_y^1 \frac{dt}{\sqrt{(1-t^2)(\kappa'^2 + \kappa^2 t^2)}} = \operatorname{cn}^{-1}(y, \kappa) \tag{6.1}$$

$$\int_y^1 \frac{dt}{\sqrt{(1-t^2)(t^2 - \kappa'^2)}} = \operatorname{dn}^{-1}(y, \kappa) \tag{6.2}$$

$$\int_0^y \frac{dt}{\sqrt{(1-t^2)(1 - \kappa^2 t^2)}} = \operatorname{sn}^{-1}(y, \kappa), \tag{6.3}$$

where the parameter κ^2 is referred to as the elliptic modulus and the parameter κ'^2, defined by $\kappa'^2 = 1 - \kappa^2$, is referred to as the complementarity elliptic modulus. Here, the elliptic modulus is restricted to the range, $0 < \kappa < 1$. $\operatorname{cn}(x, \kappa)$ and $\operatorname{sn}(x, \kappa)$ functions have real period $4K(\kappa)$, whereas $\operatorname{dn}(x, \kappa)$ has the real period $2K(\kappa)$. Here, $K(\kappa)$ is the complete elliptic integral of the first kind given by

$$K(\kappa) = \int_0^{\pi/2} \frac{1}{\sqrt{1 - \kappa^2 \sin^2(\theta)}} d\theta. \tag{6.4}$$

The complete elliptic integral of the second kind, $E(\kappa)$, involving squares of the Jacobi elliptic functions, is defined by

$$E(\kappa) = \int_0^{\pi/2} \sqrt{1 - \kappa^2 \sin^2(\theta)} d\theta = \int_0^{K(\kappa)} \operatorname{dn}^2 du. \tag{6.5}$$

Limiting values of $K(\kappa)$ and $E(\kappa)$ are listed in the following table.

function	$\kappa = 0$	$\kappa = 1$
$K(\kappa)$	$\pi/2$	∞
$E(\kappa)$	$\pi/2$	1

The limiting values of the three elementary elliptic functions are given below.

function	$\kappa = 0$	$\kappa = 1$
$\mathrm{cn}(x, \kappa)$	$\cos(x)$	$\mathrm{sech}(x)$
$\mathrm{dn}(x, \kappa)$	1	$\mathrm{sech}(x)$
$\mathrm{sn}(x, \kappa)$	$\sin(x)$	$\tanh(x)$

The Jacobi elliptic functions satisfy the algebraic relations

$$\mathrm{sn}^2(x, \kappa) + \mathrm{cn}^2(x, \kappa) = 1, \tag{6.6}$$

$$\kappa^2 \mathrm{sn}^2(x, \kappa) + \mathrm{dn}^2(x, \kappa) = 1, \tag{6.7}$$

$$\mathrm{dn}^2(x, \kappa) - \kappa^2 \mathrm{cn}^2(x, \kappa) = \kappa'^2, \tag{6.8}$$

$$\kappa'^2 \mathrm{sn}^2(x, \kappa) + \mathrm{cn}^2(x, \kappa) = \mathrm{dn}^2(x, \kappa). \tag{6.9}$$

The derivatives of the Jacobi elliptic functions are given by

$$\frac{\partial}{\partial x} \mathrm{cn}(x, \kappa) = -\mathrm{sn}(x, \kappa)\mathrm{dn}(x, \kappa), \tag{6.10}$$

$$\frac{\partial}{\partial x} \mathrm{dn}(x, \kappa) = -\kappa^2 \mathrm{cn}(x, \kappa)\mathrm{sn}(x, \kappa), \tag{6.11}$$

$$\frac{\partial}{\partial x} \mathrm{sn}(x, \kappa) = \mathrm{cn}(x, \kappa)\mathrm{dn}(x, \kappa). \tag{6.12}$$

List of Publications

1. N. Gurappa, P.K. Panigrahi, **T. Soloman Raju,** and V. Sreenivasan, "Quantum Equivalent of Bertrand's theorem", Mod. Phys. Lett. A 30 1851 (2000).

2. N. Gurappa, P.K. Panigrahi, and **T. Soloman Raju,** "On A Unified Algebraic Approach for Solving Few and Many-Body Interacting Systems", Proceedings of International Conference on Mathematical Physics, Nagpur, India 1 95-98 (2000).

3.T. **Soloman Raju** and P.K. Panigrahi, "On the Relevance of the Solitary Wave Solutions of the σ -Model to Disoriented Chiral Condensates, Proceedings of the XIV DAE Symposium on High Energy Physics, Hyderabad, India, 101-103 (2000).

4.T. Soloman Raju, C. Nagaraja Kumar, and P.K. Panigrahi, " Exact Solutions of nonlinear Schrodinger equation with a source", nlin.SI/0308012, submitted to Phys. Rev. Lett.

5. **T. Soloman Raju,** G.S. Agarwal, and P.K. Panigrahi, "Solitary Waves in Two-component Bose-Einstein Condensates in Quasi-onedimensional Geometry, To be submitted to Phys. Rev. A.

6. **T. Soloman Raju** and P.K. Panigrahi, "Exact solutions of driven NLSE with a source" To be submitted.

7. **T. Soloman Raju,** C. Nagaraja Kumar, and P.K. Panigrahi, "Compacton Solutions of MKdV and NLSE with Sources", To be submitted.

8. **T. Soloman Raju** and P.K. Panigrahi, "Phase Dynamics of Chiral order parameter and Disoriented Chiral Condensates", To be submitted.

9. T. Soloman Raju and P.K. Panigrahi, "On the Rational Solutions of Boussinesq Equation", To be submitted.